

Discovery of Inducible Nitric Oxide Synthase (iNOS) Inhibitor Development Candidate KD7332, Part 1: Identification of a Novel, Potent, and Selective Series of Quinolinone iNOS Dimerization Inhibitors that are Orally Active in Rodent Pain Models

Céline Bonnefous,[†] Joseph E. Payne,[†] Jeffrey Roppe,[†] Hui Zhuang,[†] Xiaohong Chen,[†] Kent T. Symons,[‡] Phan M. Nguyen,[‡] Marciano Sablad,[§] Natasha Rozenkrants,[§] Yan Zhang,[§] Li Wang,^{||} Daniel Severance,[†] John P. Walsh,[⊥] Nahid Yazdani,[⊥] Andrew K. Shiau,[‡] Stewart A. Noble,[†] Peter Rix,^{||} Tadimeti S. Rao,[§] Christian A. Hassig,[‡] and Nicholas D. Smith^{*†}

Department of Chemistry, Department of Biology, Department of Pharmacology, Department of Drug Metabolism and Pharmacokinetics, Department of Analytical Chemistry, Kalypsys Inc., 10420 Wateridge Circle, San Diego, CA 92121

Received February 10, 2009

There are three isoforms of dimeric nitric oxide synthases (NOS) that convert arginine to citrulline and nitric oxide. Inducible NOS is implicated in numerous inflammatory diseases and, more recently, in neuropathic pain states. The majority of existing NOS inhibitors are either based on the structure of arginine or are substrate competitive. We describe the identification from an ultra high-throughput screen of a novel series of quinolinone small molecule, nonarginine iNOS dimerization inhibitors. SAR studies on the screening hit, coupled with an in vivo lipopolysaccharide (LPS) challenge assay measuring plasma nitrates and drug levels, rapidly led to the identification of compounds **12** and **42**—potent inhibitors of the human and mouse iNOS enzyme that were highly selective over endothelial NOS (eNOS). Following oral dosing, compounds **12** and **42** gave a statistical reduction in pain behaviors in the mouse formalin model, while **12** also statistically reduced neuropathic pain behaviors in the chronic constriction injury (Bennett) model.

Introduction

Nitric oxide synthases (NOS^a) are dimeric enzymes that catalyze the formation of nitric oxide (NO) and citrulline from arginine and molecular oxygen using heme, bipterin, and NADPH as cofactors. Three isoforms of NOS have been identified: two of these, endothelial NOS (eNOS) and neuronal NOS (nNOS), are constitutively expressed and play important roles in blood pressure regulation and neurotransmission respectively. The third isoform, inducible NOS, is synthesized in response to exposure to inflammatory and immunologic stimuli and has been implicated in the pathogenesis of numerous diseases including septic shock, asthma, inflammatory bowel disease, osteoarthritis, and rheumatoid arthritis.¹ More recently, there is increasing evidence of the involvement of iNOS in the development and maintenance of neuropathic pain states.²

There has been substantial activity in the pharmaceutical industry to identify selective iNOS inhibitors, with selectivity over eNOS being particularly important as inhibition can result in an elevation of blood pressure. Much of the initial work centered on substrate competitive inhibitors structurally related to arginine. L-NNA (**1**) and L-NIL (**2**) exemplify this structural class and exhibit poor selectivity for iNOS over eNOS.³ GW271450 (**3**), a structurally related compound exhibits time-dependent inhibition, improved selectivity for iNOS over eNOS and is efficacious in preclinical models of pain.⁴ Given that

structural similarity to arginine confers risk of potential interference with physiological processes dependent on arginine transport and metabolism,⁵ we prioritized the identification and characterization of novel nonsubstrate competitive NOS inhibitors.

Small molecule iNOS inhibitors (Figure 1) that are structurally distinct from arginine have precedent and often incorporate a guanidine mimetic. For example, compound **4**, a substrate competitive inhibitor, displayed high iNOS potency and good efficacy in a rat LPS assay measuring nitrate release, however, selectivity over eNOS was poor (40-fold).⁶ Another substrate competitive inhibitor AR-C102222 (**5**), demonstrated good selectivity for iNOS over eNOS and was efficacious in a rat adjuvant-induced arthritis model and other models of neuropathic and surgical pain.⁷

More recently, BBS-4 (**6**), an imidazole-based inhibitor that is able to disrupt the formation of the active NOS dimer by direct coordination of the imidazole to the heme iron in the active site of the enzyme, was reported.⁸ Compound **6** is a potent and selective iNOS inhibitor, however, compounds that actively coordinate to heme iron have been shown to be potent inhibitors of cytochrome P450s,⁹ resulting in the potential for drug–drug interactions. NOS dimerization inhibitors that lack cytochrome P450 cross reactivity are expected to exhibit a unique in vivo profile distinct from substrate competitive inhibitors and have utility in neuropathic pain. We thus conducted a cell-based ultra high-throughput screen on a small molecule library of approximately 880000 compounds looking for nonarginine, non-imidazole-based dimerization inhibitors of iNOS. From this screen, four series of human iNOS inhibitors were identified, including a set of quinolinones represented by **7** (Figure 2). Quinolinone **7** had an EC₅₀ of 1.3 μM against human iNOS (hiNOS) and had good selectivity over human eNOS (heNOS > 70-fold), however it had poor inhibitory activity against the mouse iNOS isoform (miNOS EC₅₀ = 46 μM)—a key issue as activity against miNOS would be required for future pharmacological evaluation of the series in rodents. This paper describes

* To whom correspondence should be addressed. Phone: (858)754-3481. Fax: (858)754-3301. E-mail: nsmith@kalypsys.com.

[†] Department of Chemistry.

[‡] Department of Biology.

[§] Department of Pharmacology.

^{||} Department of Drug Metabolism and Pharmacokinetics.

[⊥] Department of Analytical Chemistry.

^a NOS, nitric oxide synthase; NO, nitric oxide; iNOS, inducible NOS; eNOS, endothelial NOS; nNOS, neuronal NOS; uHTS, ultra high-throughput screening; LPS, lipopolysaccharide; SDS-PAGE, sodium dodecyl sulfate polyacrylamide gel electrophoresis; CCI, chronic constriction injury; DAN, diamionaphthalene.

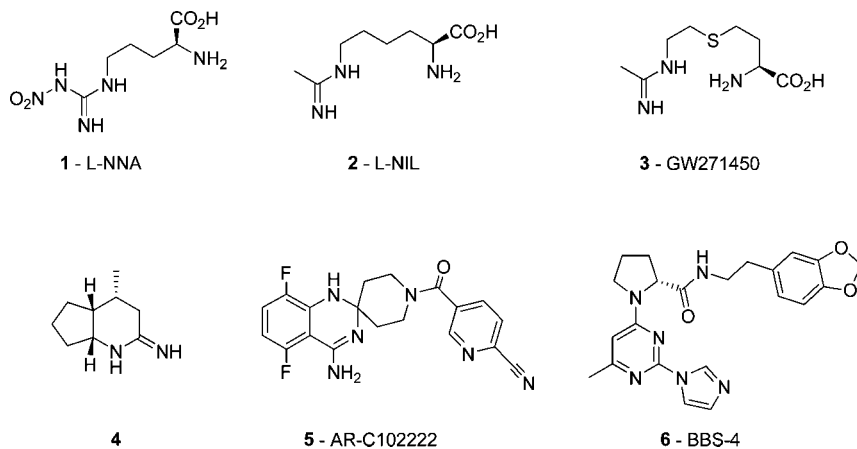


Figure 1. iNOS inhibitors.

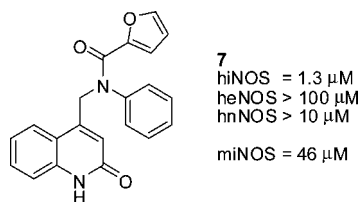
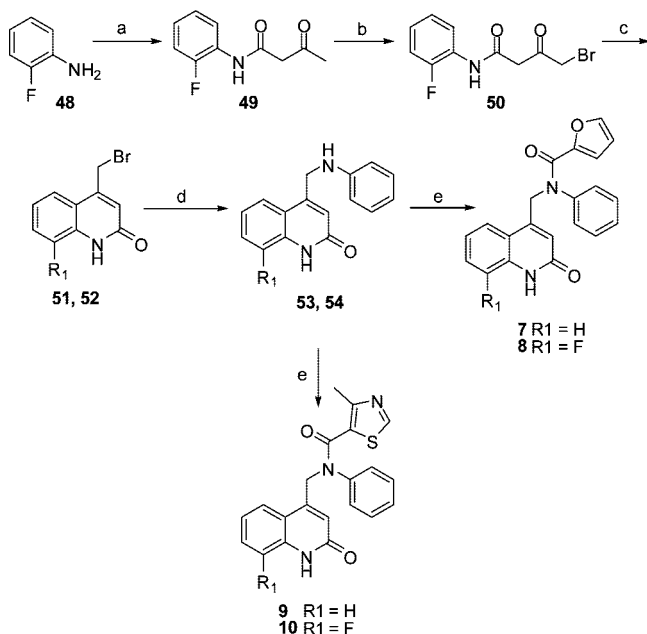


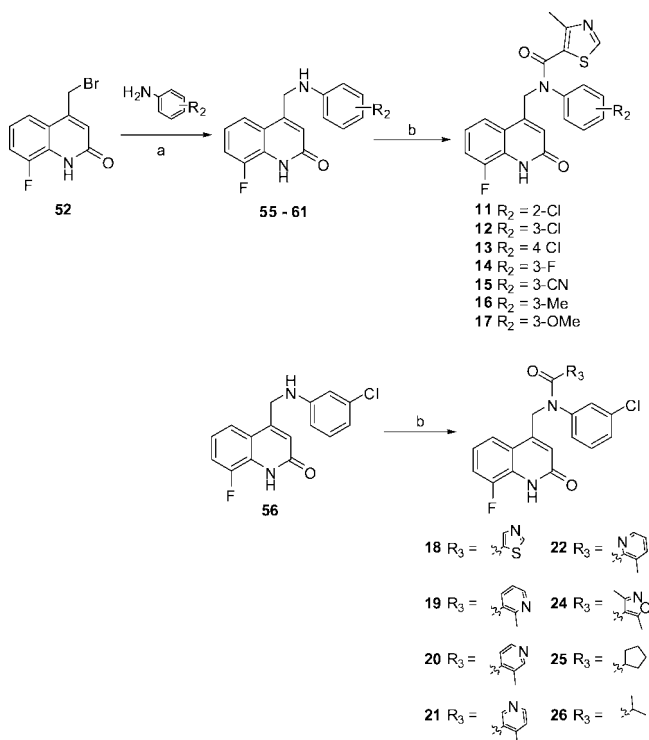
Figure 2. Ultra high-throughput screening hit quinolinone 7.

Scheme 1^a

^a Reagents and conditions: (a) Methyl 3-oxobutanoate, pyridine, xylene, reflux, 30 min. (b) (i) Bromine, AcOH, 25 °C, 5 h; (ii) acetone, 25 °C, 18 h. (c) H₂SO₄, 45 °C, 18 h. (d) Aniline, DMSO, 50 °C, 1 h. (e) (i) Carboxylic acid, oxalyl chloride, DMF, DCM, 25 °C, 2 h; (ii) DIEA, NMP, 25 °C, 14 h; (iii) propylamine, 25 °C, 30 min.

the characterization and structure–activity relationship of this quinolinone series of iNOS dimerization inhibitors and the evolution of uHTS hit 7 to potent inhibitors of human and mouse iNOS that are orally active in mouse LPS challenge, mouse formalin, and mouse chronic constriction injury models.

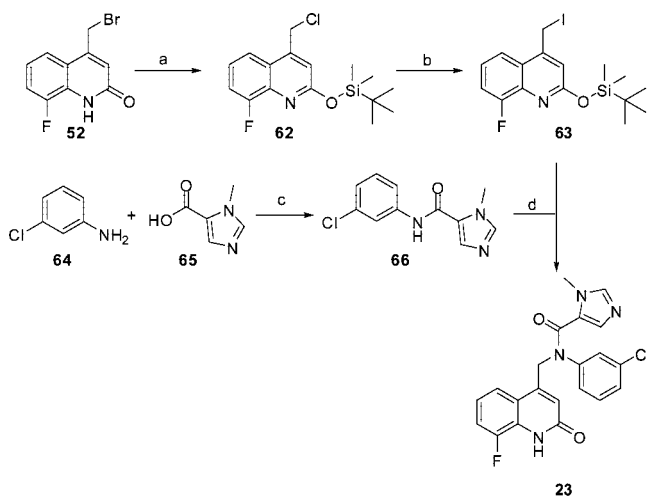
Chemistry. The synthetic route used to make uHTS hit 7 and compounds 8–10 is shown in Scheme 1. Thus keto-amide 49 formed by the reaction of fluoroaniline 48 with methyl 3-oxobutanoate, was selectively brominated at the α position¹⁰

Scheme 2^a

^a Reagents and conditions: (a) DMSO, 50 °C, 1 h. (b) (i) Carboxylic acid, oxalyl chloride, DMF, DCM, 25 °C, 2 h; (ii) DIEA, NMP, 25 °C, 14–18 h; (iii) Propylamine, 25 °C, 30 min.

to give 50. Cyclization of 50 under acidic conditions gave 8-fluoroquinolinone (52) (R₁ = F), which was reacted with aniline followed by acylation with either furan-2-carbonyl chloride or 4-methylthiazole-5-carbonyl chloride to give 8 or 10, respectively. Of note is the use of two equivalents of acylating reagent, which first alkylates the quinolinone, followed by the aniline nitrogen; addition of propylamine then removes the quinolinone acyl group to give the desired product. Similarly, starting from commercially available quinolinone 51 (R₁ = H), compounds 7 and 9 were prepared.

Scheme 2 summarizes the preparation of compounds 11–22 and 24–26. Thus substituted anilines were alkylated with 8-fluoroquinolinone (52) to give intermediates 55–61, which were subsequently acylated with 4-methylthiazole-5-carbonyl chloride to give compounds 11–17. Additionally, 3-chlorophenylamine (56) was acylated with a selection of aryl and alkyl acid chlorides to give 18–22 and 24–26.

Scheme 3^a

^a Reagents and conditions: (a) TBDMS-Cl, DMF, 25 °C, 4 h. (b) NaI, acetone, 25 °C, 2 h. (c) HATU, Et₃N, DMF, 25 °C, 18 h. (d) NaH, DMF, 25 °C, 3.5 h.

Imidazole-amide (**23**) required an alternative route from that shown in Scheme 2 for its preparation that utilized a protected quinolinone alkylating agent (Scheme 3). Thus 8-fluoroquinolinone (**52**) was protected with a tertiary-butyl dimethylsilyl group and converted to the corresponding iodide **63**. Alkylation of amide **66** with iodide **63** gave **23** (deprotection of the silyl protecting group occurred under the reaction conditions).

Compounds **27–34** that explore the SAR of the quinolinone portion of **12** required a number of diverse synthetic routes for their preparation (Schemes 4–7). Thus pyridone **27** was prepared in three steps as shown in Scheme 4: 3-chloroaniline was alkylated with **67**,¹¹ followed by acylation with 4-methylthiazole-5-carboxyl chloride to give **69**. Hydrolysis of the 2-chloropyridine of **69** in acetic acid then gave pyridone **27**. Tetrahydroquinolinone (**28**) was prepared in five steps starting from ester **70**. Thus reduction of ester **70** to alcohol **71** with LAH was followed by conversion to the benzylic bromide (**72**) with PBr₃, which in an analogous fashion to **27** was converted to tetrahydroquinolinone (**28**). Coumarin **29** was prepared from hydroxyketone **75** in four steps as shown in Scheme 4. Reaction of **75** with phosphoranylidene ester (**76**)¹² gave coumarin **77**, which was converted to the benzylbromide **78** using NBS/AIBN. Alkylation of 3-chloroaniline with **78** followed by acylation with 4-methylthiazole-5-carboxyl chloride gave **29**.

Access to methoxyquinoline (**30**) and *N*-methyl-quinolinone (**31**) is depicted in Scheme 5. Thus alkylation of **12** with NaH/dimethylsulfate gave a mixture of regioisomers which were separated to give **30** and **31**. The identity of **30** and **31** was confirmed by the independent synthesis of **30**.¹³

Compound **32** was prepared from 8-fluoroquinoline (**80**)¹⁴ in three steps as shown in Scheme 6. Quinoline benzyl bromide **81** resulting from the bromination of **80** with NBS/AIBN was reacted with 3-chloroaniline to give **82**; acylation of **82** then gave **32**.

Isoquinoline (**33**) and its *N*-oxide **34** were prepared as shown in Scheme 7. Thus palladium catalyzed cyclization¹⁵ of *ortho*-iodoalkene (**85**) gave isoquinolinone (**86**), which was deprotected and converted to 1-chloroisoquinoline (**88**) using POCl₃. Intermediate **88** was converted to benzylbromide (**89**) using NBS/AIBN, which was used to alkylate 3-chloroaniline to afford **90**. Palladium catalyzed hydrogenation led to selective reduction of the chlorine of the 1-chloroisoquinoline to give **91**, which

was acylated to give compound **33**. Oxidation of **33** with *m*-CPBA gave isoquinoline *N*-oxide (**34**).

Scheme 8 illustrates the synthesis of compounds **35–41**, **43**, and **44**, which further explores the impact of substitution on the quinolinone nucleus. Thus keto-amides **98–102** formed by the reaction of anilines **92–96** with methyl 3-oxobutanoate were selectively brominated at the α -position to give **50** and **103–107**. Using 1-chloromethyl-4-fluoro-1,4-diazoniabicyclo[2.2.2]octane bis-(tetrafluoroborate), fluorine was introduced at the 2-position of **50** (R₄ = 8-F) to give **108**, which was then cyclized in hot sulfuric acid to give quinolinone **114** (R₄ = 8-F, R₅ = F). Similarly, **103–107** were converted to quinolinones **51** and **109–113**. These quinolinone intermediates were then processed as described in Scheme 1 to give compounds **35–38**, **40**, and **44**.

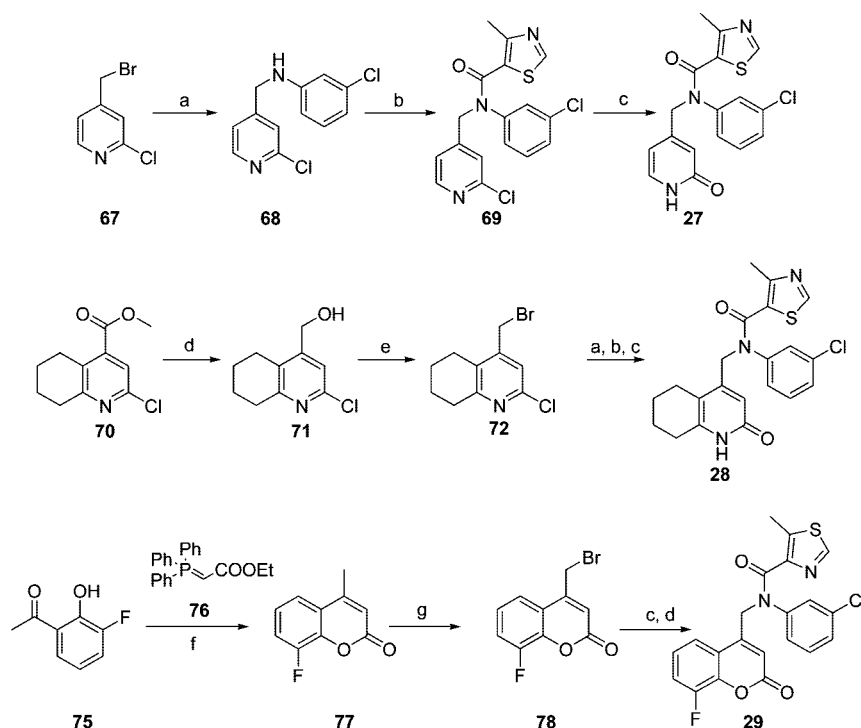
When the synthesis of 5-fluoroquinolinone derivative **39** was initially attempted using 3-fluoroaniline as a starting material, it was found that cyclization of intermediate **104** occurred at the 4-position to give undesired quinolinone **110** rather than at the 2-position to give **123** (Scheme 9). Thus to access compound **39**, the 4-position of intermediate **104** was blocked with bromine leading via intermediate quinolinone **112** (R₄ = 5-F, 8-Br, R₅ = H) to **122** (R₄ = 5-F, 8-Br, R₅ = H). Removal of bromine from **122** by hydrogenation then gave desired **39**. Compounds **41** and **43** were prepared by acylation of **120** (R₄ = 7,8-diF, R₅ = H) with the respective carbonyl chloride, while imidazole **42** was prepared as shown in Scheme 3 but using **113** (Scheme 8, R₄ = 7,8-diF, R₅ = H) in place of **52** as the starting quinolinone.

Finally, the 7,8-difluorocoumarin (**45**) was prepared as shown Scheme 4 but using 1-(3,4-difluoro-2-hydroxyphenyl)ethanone¹⁶ as the starting material, while the isoquinoline (**46**) and isoquinoline *N*-oxide (**47**) were prepared as shown in Scheme 7 but using 2,3-difluoro-6-iodobenzoic acid as the starting material.

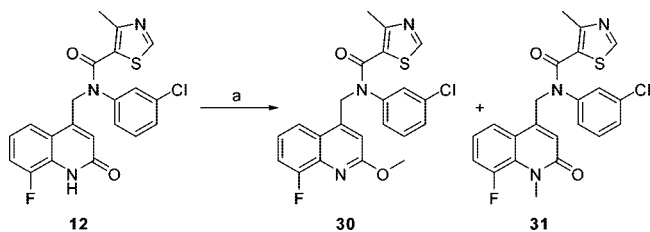
Results and Discussion

The compounds prepared in Schemes 1–8 were tested for inhibitory activity against iNOS, eNOS, and nNOS using a cell-based NOS assay using transiently transfected HEK293 cells. Nitric oxide was measured using 2,3-diaminonaphthalene with each EC₅₀ determined from three separate assay runs (each using a 10-point concentration curve). In this phenotypic cell-based assay, compounds are examined for their ability to inhibit the production of nitric oxide from the three indicated NOS isoforms. Initial SAR work was focused on changing the substituent R₁ at positions around the quinolinone core and the amide group R₂ of **7**. Selected SAR illustrating single-point changes relative to **7** is shown in Table 1. Incorporation of an 8-fluoro group on the quinolinone **8** led to a slight improvement in potency (hiNOS EC₅₀ = 1.1 μ M), while changing the 2-furylamide to a 5-thiazolyl amide (**9**) improved human iNOS potency to 0.50 μ M. Combining these two changes into a single molecule (**10**) led to an additive improvement in hiNOS potency (hiNOS EC₅₀ = 0.20 μ M) while still maintaining excellent selectivity over heNOS (>500 fold).

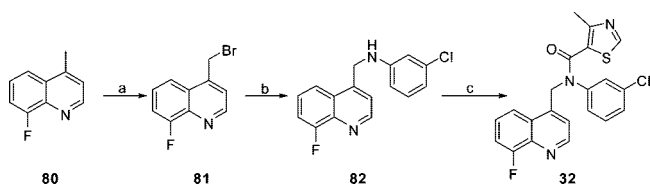
While maintaining the 8-fluoroquinolinone moiety of **10**, the SAR of the phenylamide portion of the molecule was examined as shown in Table 2. It quickly became apparent that lipophilic groups at the 3-position were favored as demonstrated by a R₁ substituent scan. Thus 2-chloro derivative **11** lost potency compared to **10**, whereas the 3-chloro **12** showed a significant increase in potency (hiNOS EC₅₀ = 0.011 μ M) while the 4-chloro derivative **13** was equipotent to **10**. When examining

Scheme 4^a

^a Reagents and conditions: (a) 3-Chloroaniline, Na₂CO₃ or K₂CO₃, DMF or DMSO, 2 h. (b) 4-Methylthiazole-5-carbonyl chloride, DMF or NMP, 25 °C. (c) AcOH, 140 °C. (d) LiAlH₄, THF, 0 °C, 30 min. (e) PBr₃, DCM 0–25 °C, 30 min. (f) **76**, toluene, 120 °C, 18 h. (g) NBS, AIBN, CCl₄, reflux, 18 h.

Scheme 5^a

^a Reagents and conditions: (a) NaH, dimethylsulfate, DCM, 25 °C, 18 h.

Scheme 6^a

^a Reagents and conditions: (a) NBS, AIBN, CCl₄, reflux, 18 h. (b) 3-Chloroaniline, K₂CO₃, DMF, 60 °C, 2 h. (c) 4-Methylthiazole-5-carbonyl chloride, NMP, 25 °C, 18 h.

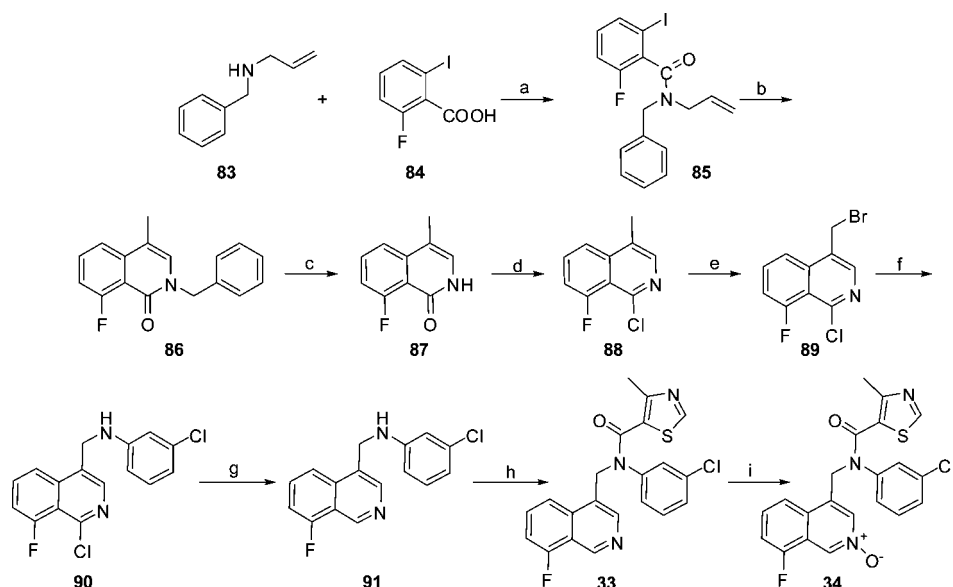
the nature of the group at the 3-position, small lipophilic groups such as 3-fluoro (hiNOS EC₅₀ = 0.062 μM), 3-cyano (hiNOS EC₅₀ = 0.056 μM), or 3-methyl (hiNOS EC₅₀ = 0.104 μM) maintained activity relative to **12**, whereas more polar groups such as 3-methoxy (hiNOS EC₅₀ = 0.99 μM) or 3-pyridyl (hiNOS EC₅₀ = 1.8 μM)¹⁷ lost significant activity.

Not only did 3-chloro derivative **12** show a greatly improved human iNOS potency, it also maintained good selectivity over human eNOS (heNOS EC₅₀ = 26 μM, 2300 fold selective) and nNOS (hnNOS EC₅₀ = 2.3 μM, 210 fold selective). Crucially, compared to uHTS hit **7** (miNOS = 46 μM), **12** was potent against the mouse iNOS enzyme (miNOS = 0.12 μM), allowing for proof of concept mouse pharmacology experiments (vide infra).

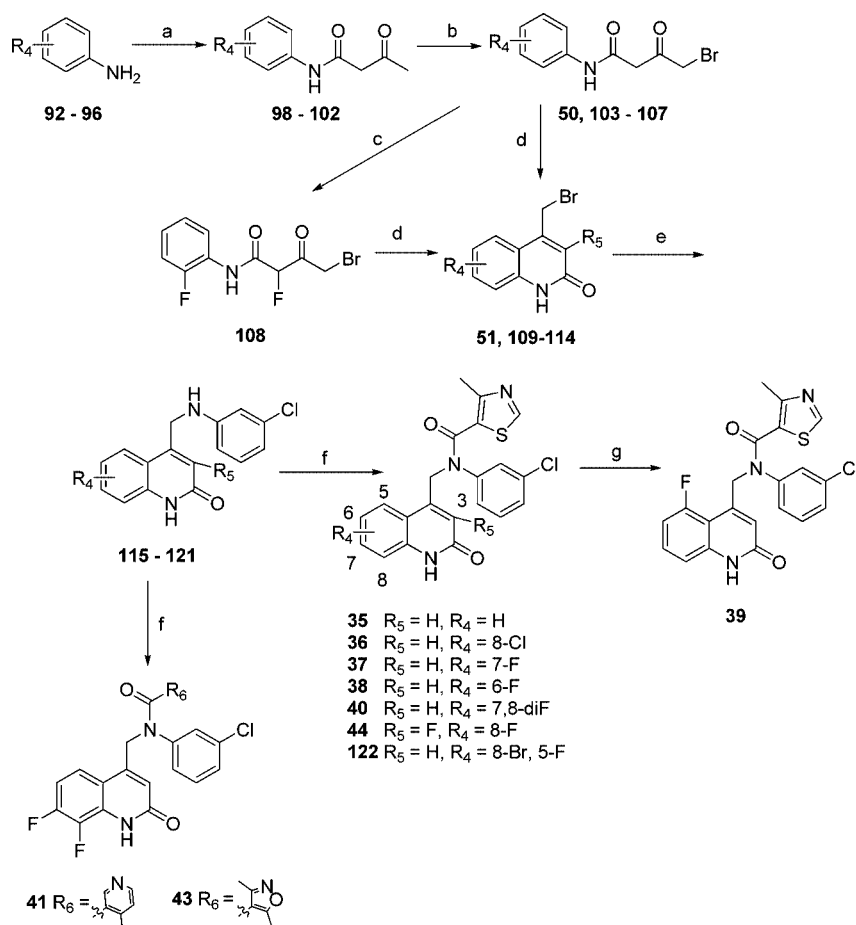
Because of the breakthrough improvements in human and mouse iNOS potency, **12** was characterized further. As illustrated in Figure 3, single crystal X-ray diffraction confirmed the structure of **12** and showed a *trans*- relationship between the thiazole and quinolinone about the amide bond.

The quaternary structure of the iNOS enzyme in the presence of **12** was investigated using low-temperature SDS-PAGE, followed by immunoblotting with antibodies recognizing the iNOS protein.¹⁸ Under these conditions, monomeric and dimeric iNOS can be resolved on the basis of having distinct mobility within the gel matrix. Enzyme isolated from cells treated with vehicle (DMSO) or substrate competitive inhibitor SEITU (50 μM)¹⁹ retained a population of dimeric iNOS (Figure 4). In contrast, compound **12** reduced the level of iNOS dimer in a concentration-dependent manner, indicating that **12** is an iNOS dimerization inhibitor (seven-point dose response; 1 μM to 0.2 nM). A similar reduction of dimer population was seen with imidazole-based dimerization inhibitor BBS-4 at 1 μM (**6**). This data suggests that **12** (and the compounds described in this paper) binds iNOS in a monomeric or loose dimeric state and interferes with the formation of a stable, enzymatically active dimer.

Having identified lead molecule **12**, we next examined the SAR of the amide region of the molecule (R₂; Table 2). It was found that the *ortho*-methyl group on the thiazole of **12** was important for potency, thus des-methyl thiazole amide **18** (hiNOS EC₅₀ = 0.053 μM) lost potency relative to **12** (hiNOS EC₅₀ = 0.011 μM), a trend that was seen for a number of other R₂ heterocyclic groups.²⁰ A pyridyl scan while fixing an *ortho*-methyl also demonstrated that the position of the heteroatom in the R₂ group was important. Thus **20** and **21** maintained activity (hiNOS EC₅₀ < 0.1 μM), whereas **19** (hiNOS EC₅₀ = 0.35 μM) and **22** (hiNOS EC₅₀ = 0.42 μM) lost significant activity relative to **12**. Incorporating these two lessons into alternative R₂ five-membered ring heterocycles led to the

Scheme 7^a

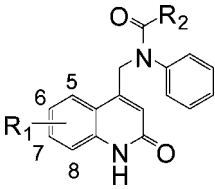
^a Reagents and conditions: (a) (i) SOCl₂, 80 °C, 1.5 h; (ii) Et₃N, THF, 5–25 °C, 2 h. (b) Dicyclohexylamine, PPh₃, Pd(OAc)₂, DMA, 100 °C, 18 h. (c) H₂SO₄, 150 °C, 2.5 h. (d) POCl₃, 80 °C, 2 h. (e) NBS, AIBN, CCl₄, reflux, 18 h. (f) 3-Chloroaniline, K₂CO₃, DMF, 60 °C, 2 h. (g) H₂, Pd/C, MeOH, 25 °C, 4 h. (h) 4-Methylthiazole-5-carbonyl chloride, NMP, 25 °C, 18 h. (i) *m*-CPBA, DCM, 25 °C, 1 h.

Scheme 8^a

^a Reagents and conditions: (a) Methyl 3-oxobutanoate, pyridine, xylene, reflux, 30 min. (b) (i) Bromine, AcOH, 25 °C, 5 h; (ii) acetone, 25 °C, 18 h. (c) 1-Chloromethyl-4-fluoro-1,4-diazoniabicyclo[2.2.2]octane bis-(tetrafluoroborate) ACN, 60 °C, 2 h. (d) H₂SO₄, 45 °C, 18 h. (e) 3-Chloroaniline, DMSO, 50 °C, 1 h. (f) (i) Carboxylic acid, oxalyl chloride, DMF, DCM, 25 °C, 2 h; (ii) DIEA, NMP, 25 °C, 14 h; (iii) propylamine, 25 °C, 30 min. (g) H₂, Pd/C, MeOH, 25 °C, 18 h.

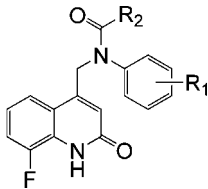
discovery of imidazole **23** (hiNOS EC₅₀ = 0.009 μM) and isoxazole **24** (hiNOS EC₅₀ = 0.016 μM), two potent human

iNOS inhibitors that still maintained good selectivity over heNOS (>400 fold). Of note is the higher selectivity for human

Table 1. Selected SAR of uHTS Hit 7


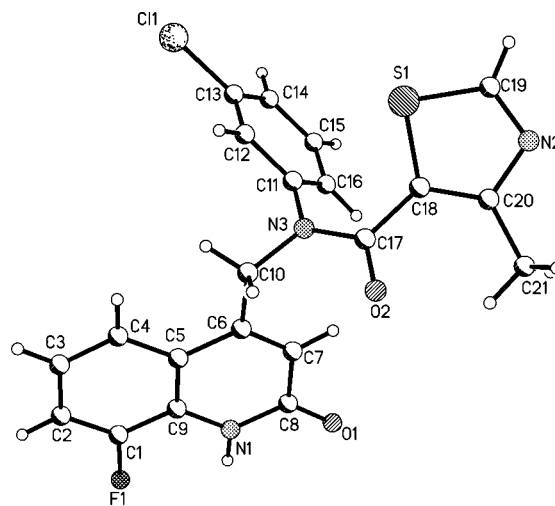
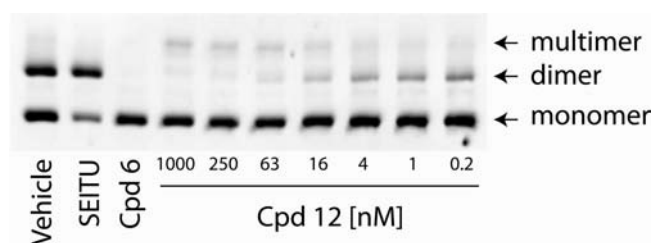
Compd	R ¹	R ²	EC ₅₀ (μM) ^a			Selectivity	
			iNOS	eNOS	nNOS	eNOS/iNOS	nNOS/iNOS
7	H		1.3 (0.36)	>100 ^b	>10 ^c	>70	>7
8	8-F		1.1 (0.19)	>100 ^b	>10 ^c	>90	>9
9	H		0.50 (0.07)	>100 ^b	>10 ^c	>200	>20
10	8-F		0.20 (0.1)	>100 ^b	>10 ^c	>500	>50

^a Cell-based NOS assay using transiently transfected HEK293 cells; NO measured using 2,3-diaminonaphthalene (DAN). Each EC₅₀ is determined from three separate assay runs, each using a 10-point concentration curve with $n = 8$ /point for iNOS and $n = 3$ /point for eNOS and nNOS. Standard deviation shown in brackets. ^b <50% inhibition @ 100 μM. ^c <50% inhibition @ 10 μM (100% being maximal inhibition of control compound 6).

Table 2. SAR of Amide (R₂) and Aryl (R₁) of Compound 10


Compd	R ¹	R ²	EC ₅₀ (μM) ^a			Selectivity	
			iNOS	eNOS	nNOS	eNOS/iNOS	nNOS/iNOS
10	H		0.20 (0.10)	>100 ^b	>10 ^c	>500	>50
11	2-Cl		13 (4.6)	>100 ^b	>10 ^c	>8	>1
12	3-Cl		0.011 (0.002)	26 (5.7)	2.3 (0.9)	2300	210
13	4-Cl		0.24 (0.05)	>100 ^b	>10 ^c	>400	>40
14	3-F		0.062 (0.01)	15 (2.6)	ND ^d	240	ND ^d
15	3-CN		0.056 (0.02)	>100 ^b	2.7 (0.3)	>1700	50
16	3-Me		0.10 (0.02)	>100 ^b	>10 ^c	>960	>95
17	3-OMe		0.99 (0.19)	>100 ^b	>10 ^c	>100	>10
18	3-Cl		0.053 (0.3)	>100 ^b	ND ^d	>1800	ND ^d
19	3-Cl		0.35 (0.05)	>100 ^b	7.9 (6.3)	>280	23
20	3-Cl		0.089 (0.02)	13 (4.5)	2.1 (0.4)	145	24
21	3-Cl		0.049 (0.01)	41 (6.8)	2.2 (0.3)	840	45
22	3-Cl		0.42 (0.1)	>100 ^b	4.1 (1.6)	>230	10
23	3-Cl		0.009 (0.003)	6.1 ^e	0.36 ^e	680	40
24	3-Cl		0.016 (0.01)	6.8 (1.4)	0.5 (0.1)	430	30
25	3-Cl		0.77 (0.08)	>100 ^b	10.3 (0.6)	>130	14
26	3-Cl		0.16 (0.02)	>100 ^b	2.9 (1.0)	>630	18

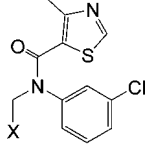
^a Cell-based NOS assay using transiently transfected HEK293 cells; NO measured using 2,3-diaminonaphthalene (DAN). Each EC₅₀ is determined from three separate assay runs, each using a 10-point concentration curve with $n = 8$ /point for iNOS and $n = 3$ /point for eNOS and nNOS. Standard deviation shown in brackets. ^b <50% inhibition @ 100 μM. ^c <50% inhibition @ 10 μM (100% being maximal inhibition of control compound 6). ^d Not determined. ^e $n = 1$ data.

**Figure 3.** Single crystal X-ray diffraction of compound 12.**Figure 4.** Compound 12 destabilizes murine iNOS dimer in cells.

iNOS over human nNOS of compound 12 (210-fold selective) relative to compounds 19–24 (10–45-fold selective). While excellent hiNOS potency was obtained with five-membered heteroaromatic R₂ groups such as 12, aliphatic cyclopentane (25) (hiNOS EC₅₀ = 0.77 μM) lost activity relative to 12. Interestingly however, when the cyclopentane was truncated to isopropyl amide (26), an improvement in potency was observed (hiNOS EC₅₀ = 0.16 μM).

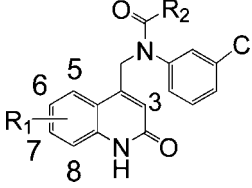
Having identified 12 through optimization of the amide and aryl ring regions of the original screening hit, we returned to examine the SAR of the quinolinone ring further using 12 as a template (Tables 3 and 4). As shown in Table 3, truncation of the quinolinone to give 27 led to a complete loss of potency, whereas saturated system 28 maintained some level of potency (hiNOS EC₅₀ = 1.14 μM).²¹ Recently, Sanofi-Aventis reported coumarin-based iNOS inhibitors,²² however, upon preparation, coumarin 29 (hiNOS EC₅₀ = 2.0 μM) was 200-fold less potent than the corresponding quinolinone 12. Further SAR examining the embedded amide of the quinolinone of 12 indicated the importance of this region of the molecule for potency against the iNOS enzyme. Thus methylation of either the oxygen (30) or nitrogen (31) or the removal of the amide as in quinoline 32 led to a complete loss of hiNOS potency. Interestingly however, isoquinoline 33 had submicromolar potency against the enzyme (hiNOS EC₅₀ = 0.76 μM), and conversion to the *N*-oxide 34 gave a further 10-fold increase in potency (hiNOS EC₅₀ = 0.087 μM). Isoquinoline *N*-oxide (34) represents a potent quinolinone replacement but one without the hydrogen bond donor capabilities of the quinolinone.

Examination of the SAR around the quinolinone ring of 12 illustrated that the size and position of the halogen greatly effected hiNOS potency (Table 4). For example, removing the 8-fluoro of 12, giving 35 or changing it to an 8-chloro (36), led to a decrease in potency of 10–100 fold. In moving the position

Table 3. SAR Examining Quinolinone Portion of Compound **12**


Compd	X	hiNOS EC ₅₀ (μM) ^a	Compd	X	hiNOS EC ₅₀ (μM) ^a
12		0.011 (0.002)	31		>100 ^b
27		>100 ^b	32		>100 ^b
28		1.14 (0.4)	33		0.76 (0.3)
29		2.0 (0.3)	34		0.087 (0.02)
30		>100 ^b			

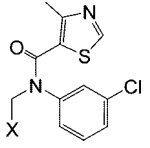
^a Cell-based NOS assay using transiently transfected HEK293 cells; NO measured using 2,3-diaminonaphthalene (DAN). Each EC₅₀ is determined from three separate assay runs, each using a 10-point concentration curve with *n* = 8/point for iNOS and *n* = 3/point for eNOS and nNOS. Standard deviation shown in brackets. ^b <50% inhibition @ 100 μM.

Table 4. Identification of a Potency-Enhancing 7,8-Difluoroquinolinone Motif


Compd	R ₁	R ₂	EC ₅₀ (μM) ^a			Selectivity	
			iNOS	eNOS	nNOS	eNOS/iNOS	nNOS/iNOS
12	8-F		0.011 (0.002)	26 (5.7)	2.3 (0.9)	2300	210
35	H		0.17 (0.05)	>100 ^b	>10 ^c	>580	>60
36	8-Cl		1.3 (0.1)	>100 ^b	>10 ^c	>75	>8
37	7-F		0.053 (0.01)	33 (5)	3.4 (3.2)	620	65
38	6-F		0.30 (0.04)	>100 ^b	>10 ^c	>330	>30
39	5-F		0.50 (0.12)	>100 ^b	>10 ^c	>200	>20
40	7,8-F		0.002 (0.001)	3.0 (0.8)	0.12 (0.03)	1500	60
41	7,8-F		0.011 (0.003)	2.5 (0.2)	0.29 (0.08)	220	25
42	7,8-F		0.003 (0.002)	0.42 (0.04)	0.07 (0.02)	140	23
43	7,8-F		0.003 (0.001)	1.2 (0.2)	0.097 (0.01)	400	32
44	3,8-F		0.026 (0.01)	35 ^d	>10 ^c	1300	>380

^a Cell-based NOS assay using transiently transfected HEK293 cells; NO measured using 2,3-diaminonaphthalene (DAN). Each EC₅₀ is determined from three separate assay runs, each using a 10-point concentration curve with *n* = 8/point for iNOS and *n* = 3/point for eNOS and nNOS. Standard deviation shown in brackets. ^b <50% inhibition @ 100 μM. ^c <50% inhibition @ 10 μM (100% being maximal inhibition of control compound **6**). ^d *n* = 1 data.

of the fluorine atom around the ring, it was found that the 7-fluoro derivative **37** (hiNOS EC₅₀ = 0.053 μM) maintained good levels of potency, while the 6- and 5-fluoro derivatives led to a decrease in potency relative to **12**. As the 7-fluoro derivative **37** increased potency relative to the unsubstituted

Table 5. Incorporation of a Difluoro Motif into Coumarin **29**, Isoquinoline **33**, and Isoquinoline *N*-oxide **34**


Compd	X	EC ₅₀ (μM) ^a			Selectivity	
		iNOS	eNOS	nNOS	eNOS/iNOS	nNOS/iNOS
45		0.84 (0.38)	ND ^b	ND ^b	ND ^b	ND ^b
46		0.20 ^c	37 ^d	>10 ^{d,e}	180	>50
47		0.019 (0.02)	34 ^d	3.2 ^d	1800	170

^a Cell-based NOS assay using transiently transfected HEK293 cells; NO measured using 2,3-diaminonaphthalene (DAN). Each EC₅₀ is determined from three separate assay runs, each using a 10-point concentration curve with *n* = 8/point for iNOS and *n* = 3/point for eNOS and nNOS. Standard deviation shown in brackets. ^b Not determined. ^c *n* = 1 data. ^d *n* = 2 data. ^e <50% inhibition @ 10 μM (100% being maximal inhibition of control compound **6**).

quinolinone **35**, we prepared 7,8-difluoroquinolinone **40** and were pleased to see a further increase in potency (hiNOS EC₅₀ = 0.002 μM) compared to **12**. Additionally, when this 7,8-disubstituted quinolinone motif was combined with other potent R₂ groups identified previously, giving pyridine **41**, imidazole **42**, and isoxazole **43**, a corresponding increase in potency was observed, leading to a series of very potent hiNOS inhibitors (hiNOS EC₅₀s < 0.010 μM). These 7,8-difluoroquinolinone derivatives still maintained good selectivity over heNOS (100–1500-fold), although it was noted that in general selectivity was eroded compared to the corresponding monofluoro derivatives (400–2300-fold). Further, the 7,8-difluoroquinolinone derivatives showed moderately lower selectivity for human iNOS over human nNOS, i.e., compound **40** (60-fold selective) versus **12** (210-fold) and **42** (23-fold selective) versus **23** (40-fold). We also prepared the 3,8-difluoroquinolinone derivative **44**, however, with an EC₅₀ = 0.026 μM, this did not show an improvement in potency compared to **12**.

Having identified a 7,8-difluoro substitution pattern on the quinolinone moiety as being optimal for potency, we installed this same fluorine substitution pattern on the coumarin and isoquinolines described in Table 3. As shown in Table 5, 7,8-difluorocoumarin (**45**), -isoquinoline (**46**), and -isoquinoline *N*-oxide (**47**) all show a 3–5-fold increase in hiNOS potency relative to the corresponding monofluoro derivative (**29**, **33**, and **34**; Table 3). Once again, isoquinoline *N*-oxide **47** is a potent quinolinone replacement, demonstrating excellent hiNOS potency (hiNOS EC₅₀ = 0.019 μM) and selectivity over human eNOS (1800-fold) and nNOS (170-fold).

In Vivo Characterization: Mouse LPS Assay. As described in Tables 1–5, SAR studies on uHTS hit **7** led to the identification of a large number of potent human iNOS inhibitors. As the SAR evolved during the course of the project, we utilized a LPS challenge assay²³ to confirm that the increases seen in in vitro iNOS potency translated to increases in in vivo activity, as determined by measuring a biomarker (NO) reflective of activity in mechanism. To further leverage this LPS challenge assay, we obtained drug levels and so looked to establish a PK–PD relationship, enabling us to effectively triage compounds. In this LPS assay, test articles (30 mpk) or vehicle control were administered orally at *t* = 0 h, followed im-

Table 6. Reduction of Plasma Nitrate Levels by Selected Compounds Following LPS Challenge^a

compd	hiNOS EC ₅₀ (μM)	miNOS EC ₅₀ (μM)	% nitrates rdn @ 30 mg/kg po (%) ^b	drug plasma @ 6 h (ng/mL)	LPS ED ₅₀ (mg/kg) po
42	0.003 (0.002)	0.014 (0.001)	95	18	5
41	0.011 (0.003)	0.057 (0.02)	95	63	16
12	0.011 (0.002)	0.12 (0.01)	90	77	10
23	0.009 (0.003)	0.034 (0.03)	67	7	13
43	0.003 (0.001)	0.022 (0.001)	67	BLQ ^c	ND ^d
40	0.002 (0.001)	0.032 (0.01)	62	8	13
44	0.026 (0.01)	0.13 (0.12)	29	BLQ ^c	ND ^d
34	0.087 (0.02)	0.66 (0.25)	20	39	ND ^d
47	0.019 (0.02)	0.074 (0.004)	10	20	ND ^d
26	0.16 (0.02)	2.7 (0.6)	6	21	ND ^d

^a Compounds administered at $t = 0$ h (30 mg/kg po) immediately followed by LPS (10 mg/kg ip). Plasma nitrate and drug levels measured at $t = 6$ h.
^b % Reduction compared to vehicle control. ^c Below limits of quantification. ^d Not determined.

mediately by injection of LPS (10 mpk ip). At $t = 6$ h, a time corresponding to peak nitrate induction, nitrate and drug levels were measured in plasma, with the reduction in nitrate levels compared to vehicle indicating the level of iNOS inhibition. Clearly, potency against the mouse iNOS enzyme was crucial for the assessment of compounds in rodent pharmacology experiments such as the LPS challenge assay. Importantly, as shown for a selection of compounds in Table 6, mouse iNOS potency did increase proportionally as human iNOS potency was optimized. It should be noted though that the compounds are 5–10-fold less potent against the mouse iNOS enzyme than the human iNOS enzyme—a trend that was observed for all the compounds in this series.

As is evident on inspection of Table 6, an in vitro potency/PK/PD correlation is generally observed. Compounds **42**, **41**, and **12** exhibit near complete reduction in plasma nitrate levels (>90%) consistent with high miNOS potency and favorable exposure, as assessed by circulating drug levels (>20ng/mL) at 6 h. In contrast, compounds **23**, **43**, and **30**, despite having good potency against mouse iNOS (miNOS EC₅₀ < 0.035 μM), achieve lower levels of plasma nitrate reduction (~65%) due to less favorable oral exposure (in each case drug levels at 6 h postdose are <10 ng/mL). Finally, as predicted, compounds with low potency against mouse iNOS, with moderate drug levels at 6 h (**34**, **26**) perform poorly in reducing circulating nitrate levels (<30% reduction). For compounds **42**, **41**, **12**, **23**, and **40**, a full dose response in the LPS challenge assay was carried out, with **42** and **12** attaining ED₅₀s following oral dosing of 5 and 10 mg/kg, respectively. This assay was used to triage >35 compounds and identified **42** and **12** as compounds for further profiling.

Mouse pharmacokinetics was carried out on **12** and **42** (Table 7) and showed that the compounds were orally bioavailable with C_{max}s (10 mg/kg po) of 1.4 and 2.2 μM, respectively. These plasma levels are 12× and 150× the respective mouse iNOS EC₅₀s, meaning that **12** and **42** were good tools for carrying out proof-of-concept studies in rodent models of pain (vide infra).

Despite achieving good plasma concentrations after oral dosing, both molecules suffered from high clearance (Cl_p > 100 mL/min/kg), suggesting these molecules would not be capable of sustained duration of action in pharmacology models. As part of an effort to understand the mechanism of clearance, compound **12** was incubated under conditions of either NADPH-dependent oxidation (NADPH only), UGT-dependent glucuronide conjugation (UGT only), or combined NADPH and UGT activities (NADPH+UGT) (Figure 5). The results clearly demonstrate that oxidation and glucuronide conjugation both contribute to the in vitro clearance of **12**. Further SAR studies on the quinolinone series utilizing this assay led to the identification of iNOS inhibitors with high metabolic stability

and good rodent and nonhuman primate pharmacokinetics; these results will be discussed in a future publication.

Inhibition values against the five major cytochrome P450 isoforms for **12** and **42** as well as other representative compounds from the series are shown in Table 8. In general, the series showed minimal inhibition of CYP's 1A2, 2D6, 2C9, and 2C19 (EC₅₀'s > 10 μM), with only CYP3A4 inhibition being in the 1–10 μM range. Compounds **12** and **42** were also profiled in a hERG patch clamp assay and determined to have EC₅₀ values of 12 and 8 μM, respectively.

Mouse Models of Pain: Formalin and Chronic Constriction Injury Models. We investigated the ability of compounds **12** and **42** to reduce pain behaviors in a mouse formalin model of nociceptive pain.²⁴ In this model, upon injection of formalin into the hind paw, a biphasic pain response is induced. The duration of pain behaviors displayed by the injured paw is then counted, with phase II being from 25–45 min postformalin injection. The duration of pain behaviors evoked in phase II are believed to involve the central sensitization of spinal neurons.²⁵ From Figure 6, it can be seen that compounds **12** and **42** (100 mg/kg po, 30 min predose to formalin challenge) both statistically reduced phase II pain behaviors in the mouse formalin model (~40% and ~65% reduction, respectively) relative to vehicle treated animals, consistent with these compounds reducing or blocking the development of central sensitization.²⁶ The attenuation of these formalin induced pain behaviors by compound **12** was not sensitive to the opiate antagonist naloxone, thereby suggesting a lack of involvement of an opiate mechanism in this response.

Compound **12** was also examined in the chronic constriction injury (CCI) model of peripheral neuropathy in which the sciatic nerve is loosely ligated, leading to spontaneous pain behaviors such as guarding or licking of the injured paw.²⁷ Additionally, allodynia and hyperalgesia due to mechanical and thermal stimuli may be observed.

As shown in Figure 7, compound **12** (100 mg/kg po, 30 min prior to testing) gave a statistically significant reduction (~45%) in the duration of pain behaviors induced by application of acetone to the injured paw (cold allodynia modality). This result indicates that **12** is orally active in a rodent model of peripheral neuropathy.

Conclusion

From an ultrahigh throughput screen we identified a novel series of quinolinone iNOS dimerization inhibitors exemplified by compound **7** (hiNOS EC₅₀ = 1.3 μM; miNOS EC₅₀ = 46 μM). SAR studies on compound **7** led to a number of potent human iNOS inhibitors (hiNOS EC₅₀ < 0.01 μM) that maintained good selectivity over eNOS and also demonstrated a corresponding increase in mouse iNOS potency (miNOS EC₅₀

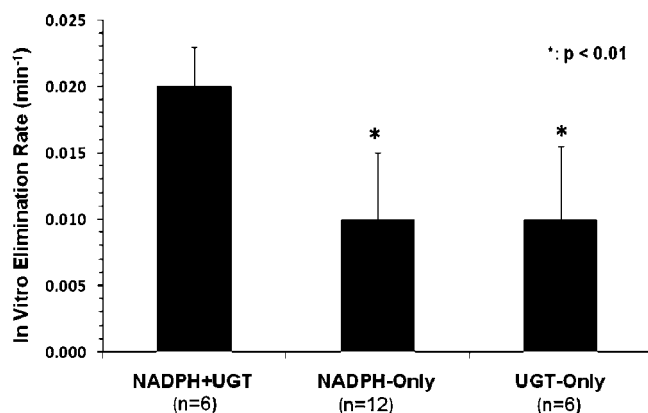


Figure 5. Elimination rate of compound **12** under conditions of combined phase I oxidation and phase II glucuronide conjugation and each separately.

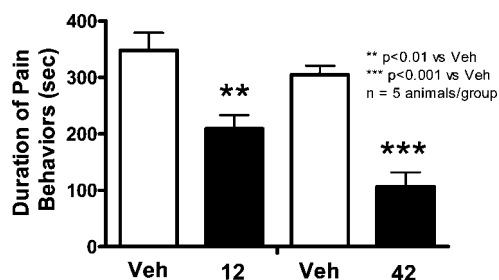


Figure 6. Compounds **12** and **42** reduce phase II pain behaviors in a mouse formalin model.

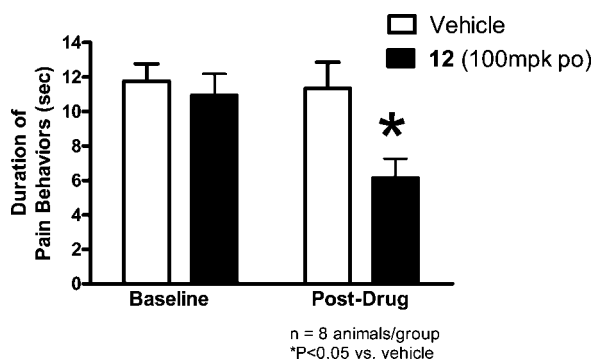


Figure 7. Compound **12** reduces pain behaviors in the chronic constriction injury model.

< 0.05 μM). These compounds were efficiently triaged utilizing a mouse LPS challenge assay measuring plasma nitrates and drug levels and led to the identification of **12** (human iNOS EC_{50} = 0.011 μM ; mouse LPS ED_{50} = 10 mg/kg po) and **42** (human iNOS EC_{50} = 0.003 μM ; mouse LPS ED_{50} = 5 mg/kg po) as lead molecules. In contrast to the majority of previously reported iNOS inhibitors, compound **12** is structurally unrelated to arginine and was confirmed to function as an iNOS enzyme dimerization inhibitor. Further, **12** and **42** were found to have minimal cross-reactivity with cytochrome P450 enzymes and the hERG channel. Despite having high clearance in vivo, compounds **12** and **42** achieved good per oral C_{max} s and were tested in mouse models of neuropathic pain. Following oral dosing, compounds **12** and **42** gave a statistical reduction in pain behaviors in the mouse formalin model (central sensitization model), while **12** also statistically reduced pain behaviors in the chronic constriction injury model (peripheral neuropathy model). In summary, we have identified a new class of highly potent, small molecule, nonarginine iNOS dimerization inhibi-

tors that display excellent selectivity over eNOS and that are orally active in rodent pain models. Future publications will address the high clearance of the quinolinone series and the subsequent evolution of the series to a clinical development candidate.

Experimental Section

Chemistry. All reactions were carried out under a nitrogen atmosphere. All solvents and reagents were obtained from commercial sources (unless otherwise specified) and used without further purification. All yields reported are not optimized. Silica gel column chromatography was carried out on either a Jones Chromatography Flashmaster II or an Isco Combiflash Companion XL using prepacked silica gel columns. Reversed-phase semipreparative HPLC purifications were carried out using a Shimadzu Discovery VP system with a SPD-20A prominence UV/vis detector (190–700 nm range). The columns used were either a Waters SunFire C18 (19 mm \times 150 mm) or a YMC-Pack Pro ODS-A (20 mm \times 150 mm) with a ACN/ H_2O solvent mixture stabilized with 0.1% TFA. Proton nuclear magnetic resonances (^1H NMR) and carbon nuclear magnetic resonances (^{13}C NMR) were recorded on a Varian 400 MHz Mercury 400VX, and the chemical shifts are reported in parts per million (δ) from an internal standard of residual DMSO (2.50 ppm, 39.5 ppm), methanol (3.31 ppm, 49.0 ppm), or chloroform (7.26 ppm, 77.2 ppm). Proton chemical data are reported as follows: chemical shift, multiplicity (s = singlet, d = doublet, t = triplet, m = multiplet, b = broad), integration, coupling constant. Analytical HPLC (for purity determination) were performed on an Agilent (1100 Series): 1 mg/mL in methanol, 5 μL injection, 254 nm detection, 1 mL/min, 1–95% ACN + 0.05% TFA/ H_2O + 0.05% TFA gradient, 15 min. Compound purity was determined as $\geq 95\%$ purity by this method. Low-resolution mass spectra (LRMS) were recorded on either a WatersMicromass ZQ or a Waters Acuity (ultra high performance LC) system using electrospray positive ionization. High-resolution mass spectra (HRMS) were obtained on a Waters LCT Premier time-of-flight mass spectrometer using electrospray positive or negative ionization. Exact masses are calculated by MassLynx(c) using the method of calculation based on a published procedure.²⁸ Melting points were measured on Mettler Toledo FP62 automated melting point apparatus using glass capillary tubes and are uncorrected.

***N*-(2-Fluorophenyl)-3-oxobutanamide (49).** A solution of methyl 3-oxobutanoate (54 mL, 0.5 mol) in xylene/pyridine (200 mL/5 mL) was heated to gentle reflux for 0.5 h. 2-Fluoroaniline (**48**, 40.0 g, 0.36 mol) was then added dropwise into the above reaction mixture and it was refluxed for 8 h, with removal of distillate through a Dean–Stark tube. The solution was allowed to cool to 25 $^\circ\text{C}$ and was extracted with 20 g of NaOH in 150 mL of H_2O . The aqueous layer was separated and made weakly acidic with concentrated HCl. The resulting precipitate was collected by filtration, washed with H_2O , and dried to give 28 g (38%) of *N*-(2-fluorophenyl)-3-oxobutanamide (**49**) as a white crystalline solid. LRMS m/z : calcd for $\text{C}_{10}\text{H}_9\text{FNO}_2$ 195.0, found 196.0 [$\text{M} + \text{H}$]⁺.

4-Bromo-*N*-(2-fluorophenyl)-3-oxobutanamide (50). Bromine (7.9 mL, 1.1 equiv) was added dropwise via an addition funnel to a solution of *N*-(2-fluorophenyl)-3-oxobutanamide (**49**, 27.2 g, 0.14 mol) in AcOH (100 mL). The resulting solution was stirred at 25 $^\circ\text{C}$ for 5 h. Acetone (10 mL) was then added and the solution was stirred at 25 $^\circ\text{C}$ for 18 h. The mixture was then concentrated to $\sim 20\%$ volume and worked up via EtOAc/ H_2O extraction. Purification by silica gel column chromatography (10% to 20% EtOAc/hexanes) afforded 26 g (68% yield) of 4-bromo-*N*-(2-fluorophenyl)-3-oxobutanamide (**50**). ^1H NMR (400 MHz, CDCl_3) δ 8.77 (s, 1H), 8.23 (t, 1H, J = 8.0 Hz), 7.11 (m, 3H), 4.07 (s, 2H), 3.85 (s, 2H). LRMS m/z : calcd for $\text{C}_{10}\text{H}_9\text{BrFNO}_2$ 272.9, found 273.8 [$\text{M} + \text{H}$]⁺.

4-(Bromomethyl)-8-fluoroquinolin-2(1H)-one (52). A mixture of 4-bromo-*N*-(2-fluorophenyl)-3-oxobutanamide (**50**, 26 g, 95 mmol) and concentrated H_2SO_4 (100 mL) was heated to 45 $^\circ\text{C}$ for 18 h. After cooling to 25 $^\circ\text{C}$, the solution was poured into ice water. The solid was filtered, washed with water, 10% aqueous sodium

bicarbonate, and again with water to give 15 g (65%) of 4-(bromomethyl)-7,8-difluoroquinolin-2(1*H*)-one (**52**) as an off-white solid. ¹H NMR (400 MHz, DMSO-*d*₆) δ 11.81 (s, 1H), 7.65 (d, 1H, *J* = 8.0 Hz), 7.44 (t, 1H, *J* = 8.1 Hz), 7.22 (m, 1H), 6.80 (s, 1H), 4.89 (s, 2H). LRMS *m/z*: calcd for C₁₀H₇BrFNO 254.9, found 256.1 [M + H]⁺.

4-((Phenylamino)methyl)quinolin-2(1*H*)-one (53). A mixture of 4-(bromomethyl)quinolin-2(1*H*)-one (**51**, commercially available, 200 mg, 0.84 mmol) and aniline (90 mg, 0.97 mmol) in DMSO (15 mL) was stirred at 50 °C for 1 h. The reaction mixture was cooled to 25 °C and poured into ice water (100 mL). The resulting precipitate was collected via vacuum filtration. The filter cake was washed with 0.1 N HCl (3 × 10 mL) and water (50 mL) to afford 100 mg (48%) of 4-((phenylamino)methyl)quinolin-2(1*H*)-one (**53**) as a yellow solid. LRMS *m/z*: calcd for C₁₆H₁₄N₂O 250.1, found 251.0 [M + H]⁺.

8-Fluoro-4-((phenylamino)methyl)quinolin-2(1*H*)-one (54). Compound **54** was synthesized as described for **53** using 4-(bromomethyl)-8-fluoroquinolin-2(1*H*)-one (**52**) and aniline as starting materials. ¹H NMR (400 MHz, DMSO-*d*₆) δ 11.61 (s, 1H), 7.62 (d, 1H, *J* = 8.0 Hz), 7.37 (ddd, 1H, *J* = 10.8, 7.6, 0.8 Hz), 7.13 (m, 1H), 7.01 (m, 2H), 6.51 (m, 3H), 6.40 (s, 1H), 6.25 (m, 1H), 4.46 (s, 2H). LRMS *m/z*: calcd for C₁₆H₁₃FN₂O 268.1, found 269.2 [M + H]⁺.

***N*-((2-oxo-1,2-dihydroquinolin-4-yl)methyl)-*N*-phenylfuran-2-carboxamide (7)**. Oxalyl chloride (86 μL, 1.0 mmol) was added to a solution of furan-2-carboxylic acid (94 mg, 0.84 mmol) and catalytic DMF (7 μL, 0.084 mmol) in DCM (10 mL) at 25 °C. The resulting mixture was stirred for 2 h, after which time it was concentrated to dryness under reduced pressure and redissolved in NMP (2 mL). The resulting solution was added at 25 °C to a separate mixture of 4-((phenylamino)methyl)quinolin-2(1*H*)-one (**53**, 100 mg, 0.4 mmol) and DIEA (350 μL, 2.0 mmol) in NMP (3 mL). After 14 h, the reaction mixture was treated with neat propylamine (100 μL, 1.2 mmol), stirred for an additional 30 min at 25 °C, and purified via reversed-phase semipreparative HPLC (ACN:H₂O + 0.1% TFA) to afford 40 mg (30%) of *N*-((2-oxo-1,2-dihydroquinolin-4-yl)methyl)-*N*-phenylfuran-2-carboxamide (**7**) as a white solid. HPLC: *t*_R = 6.30 (>99%); mp = 249.4 °C. ¹H NMR (400 MHz, DMSO-*d*₆) δ 11.71 (s, 1H), 7.82 (s, 1H, *J* = 7.6 Hz), 7.68 (s, 1H), 7.49 (td, 2H, *J* = 8.4, 1.2 Hz), 7.38–7.29 (m, 4H), 7.21–7.18 (m, 2H), 6.40 (m, 1H), 6.29 (s, 1H), 5.88 (d, 1H, *J* = 3.7 Hz), 5.26 (s, 2H). ¹³C NMR (400 MHz, DMSO-*d*₆) δ 161.9, 159.1, 146.9, 146.5, 146.2, 142.4, 139.5, 131.3, 130.2, 128.7, 128.3, 124.7, 122.6, 120.9, 118.3, 117.4, 116.4, 112.1, 50.8. LRMS (ESI⁺)/HRMS (ESI⁻) *m/z*: calcd for C₂₁H₁₆N₂O₃ 345.1, found 345.5 [M + H]⁺/343.1083 found 343.1085 [M - H]⁻.

***N*-((8-Fluoro-2-oxo-1,2-dihydroquinolin-4-yl)methyl)-*N*-phenylfuran-2-carboxamide (8)**. Compound **8** was synthesized as described for **7** using 8-fluoro-4-((phenylamino)methyl)quinolin-2(1*H*)-one (**54**) and furan-2-carboxylic acid as starting materials; HPLC: *t*_R = 6.36 (>94%); mp = 247.3 °C. ¹H NMR (400 MHz, DMSO-*d*₆) δ 11.74 (s, 1H), 7.69 (m, 1H), 7.66 (d, 1H, *J* = 8.4 Hz), 7.49–7.33 (m, 4H), 7.22–7.18 (m, 3H), 6.39 (m, 1H), 6.36 (s, 1H), 5.87 (d, 1H, *J* = 3.6 Hz), 5.26 (s, 2H). ¹³C NMR (400 MHz, DMSO-*d*₆) δ 160.8, 158.4, 149.0 (d, *J* = 244 Hz, F coupling), 146.1, 145.6 (d, *J* = 2.2 Hz), 145.5, 141.6, 129.5 (2C), 128.0, 127.6, 127.5 (2C), 121.7 (d, *J* = 7.3 Hz), 121.5, 119.8 (d, *J* = 3.6 Hz), 119.7 (d, *J* = 2.9 Hz), 116.7, 115.7 (d, *J* = 16.8 Hz), 111.4, 50.1. LRMS (ESI⁺)/HRMS (ESI⁻) *m/z*: calcd for C₂₁H₁₅FN₂O₃ 363.1, found 363.5 [M + H]⁺/361.0989 found 361.0985 [M - H]⁻.

4-Methyl-*N*-((2-oxo-1,2-dihydroquinolin-4-yl)methyl)-*N*-phenylthiazole-5-carboxamide (9). Compound **9** was synthesized as described for **7** using 4-((phenylamino)methyl)quinolin-2(1*H*)-one (**53**) and 4-methylthiazole-5-carboxylic acid as starting material; HPLC: *t*_R = 6.20 (>95%); mp = 281.6 °C. ¹H NMR (400 MHz, DMSO-*d*₆) δ 11.75 (s, 1H), 8.89 (s, 1H), 7.84 (d, 1H, *J* = 8.0 Hz), 7.51 (td, 2H, *J* = 8.4, 1.2 Hz), 7.31–7.20 (m, 4H), 7.15 (m, 2H), 6.31 (s, 1H), 5.33 (s, 2H), 2.48 (s, 3H). ¹³C NMR (400 MHz, DMSO-*d*₆) δ 162.8, 161.1, 155.4, 155.1, 145.7, 141.2, 138.8, 130.6, 129.2 (2C), 127.8, 127.6 (2C), 124.3, 123.9, 121.8, 120.2, 117.5,

115.7, 49.7, 16.6. LRMS (ESI⁺)/HRMS (ESI⁻) *m/z*: calcd for C₂₁H₁₇N₃O₂S 376.1, found 376.5 [M + H]⁺/374.0963 found 374.0959 [M - H]⁻.

***N*-((8-Fluoro-2-oxo-1,2-dihydroquinolin-4-yl)methyl)-4-methyl-*N*-phenylthiazole-5-carboxamide (10)**. Compound **10** was synthesized as described for **7** using 8-fluoro-4-((phenylamino)methyl)quinolin-2(1*H*)-one (**54**) and 4-methylthiazole-5-carboxylic acid as starting materials; HPLC: *t*_R = 6.13 (>92%); mp > 300 °C. ¹H NMR (400 MHz, DMSO-*d*₆) δ 11.75 (s, 1H), 8.89 (s, 1H), 7.68 (d, 1H, *J* = 8.0 Hz), 7.44 (m, 1H), 7.29–7.16 (m, 4H), 7.14 (m, 2H), 6.38 (s, 1H), 5.33 (s, 2H), 2.49 (s, 3H). LRMS (ESI⁺)/HRMS (ESI⁻) *m/z*: calcd for C₂₁H₁₆FN₃O₂S 394.1, found 394.6 [M + H]⁺/392.0869 found 392.0870 [M - H]⁻.

***N*-((2-Chlorophenyl)-*N*-((8-fluoro-2-oxo-1,2-dihydroquinolin-4-yl)methyl)-4-methylthiazole-5-carboxamide (11)**. Compound **11** was synthesized as described for compound **7** using 4-((2-chlorophenylamino)methyl)-8-fluoroquinolin-2(1*H*)-one (**55**) and 4-methylthiazole-5-carboxylic acid as starting materials; HPLC: *t*_R = 6.46 (>97%); mp = 273.0 °C. ¹H NMR (400 MHz, DMSO-*d*₆) δ 11.79 (s, 1H), 8.86 (s, 1H), 7.71 (d, 1H, *J* = 8.0 Hz), 7.47–7.41 (m, 2H), 7.35–7.28 (m, 3H), 7.20 (m, 1H), 6.36 (s, 1H), 5.50 (d, 1H, *J* = 15.6 Hz), 4.92 (d, 1H, *J* = 15.6 Hz), 2.49 (s, 3H). LRMS (ESI⁺)/HRMS (ESI⁻) *m/z*: calcd for C₂₁H₁₅ClFN₃O₂S 428.1, found 428.5 [M + H]⁺/428.0636 found 428.0641 [M + H]⁺.

***N*-((3-Chlorophenyl)-*N*-((8-fluoro-2-oxo-1,2-dihydroquinolin-4-yl)methyl)-4-methylthiazole-5-carboxamide (12)**. Compound **12** was synthesized as described for compound **7** using 4-((3-chlorophenylamino)methyl)-8-fluoroquinolin-2(1*H*)-one (**56**) and 4-methylthiazole-5-carboxylic acid as starting materials; HPLC: *t*_R = 6.56 (100%); mp = 201.9 °C. ¹H NMR (DMSO-*d*₆) δ 11.75 (s, 1H), 8.92 (s, 1H), 7.65 (d, 1H, *J* = 8.4 Hz), 7.47–7.41 (m, 2H), 7.30–7.19 (m, 3H), 7.07 (dt, 1H, *J* = 8.0, 1.3 Hz), 6.41 (s, 1H), 5.34 (s, 2H), 2.42 (s, 3H). ¹³C NMR (400 MHz, DMSO-*d*₆) δ 163.5, 161.6, 156.6, 156.2, 149.7 (d, *J* = 245 Hz, F coupling), 146.1, 143.3, 134.0, 131.5, 128.6, 128.4 (d, *J* = 13.9 Hz), 128.1, 127.4, 124.7, 122.4 (d, *J* = 7.3 Hz), 122.1, 120.6 (d, *J* = 2.9 Hz), 120.3 (d, *J* = 2.9 Hz), 116.6 (d, *J* = 16.9 Hz), 50.4, 17.4. LRMS (ESI⁺)/HRMS (ESI⁻) *m/z*: calcd for C₂₁H₁₅ClFN₃O₂S 428.1, found 428.5 [M + H]⁺/426.0480 found 426.0486 [M - H]⁻.

***N*-((4-Chlorophenyl)-*N*-((8-fluoro-2-oxo-1,2-dihydroquinolin-4-yl)methyl)-4-methylthiazole-5-carboxamide (13)**. Compound **13** was synthesized as described for compound **7** using 4-((4-chlorophenylamino)methyl)-8-fluoroquinolin-2(1*H*)-one (**57**) and 4-methylthiazole-5-carboxylic acid as starting materials; HPLC: *t*_R = 6.22 (100%); mp = 146.4 °C. ¹H NMR (400 MHz, DMSO-*d*₆) δ 11.77 (s, 1H), 8.92 (s, 1H), 7.66 (d, 1H, *J* = 8.0 Hz), 7.44 (dd, 1H, *J* = 11.2, 8.8 Hz), 7.35 (m, 2H), 7.22 (m, 3H), 6.38 (s, 1H), 5.32 (s, 2H), 2.42 (s, 3H). ¹³C NMR (400 MHz, DMSO-*d*₆) δ 162.7, 160.8, 155.8, 155.5, 149.0 (d, *J* = 245 Hz, F coupling), 145.4, 140.0, 132.2, 129.5 (2C), 129.3 (2C), 127.7 (d, *J* = 13.2 Hz), 123.9, 121.7 (d, *J* = 7.3 Hz), 121.6, 119.8 (d, *J* = 3.7 Hz), 119.6 (d, *J* = 2.9 Hz), 115.8 (d, *J* = 16.9 Hz), 49.7, 16.7. LRMS (ESI⁺)/HRMS (ESI⁻) *m/z*: calcd for C₂₁H₁₅ClFN₃O₂S 428.1, found 428.2 [M + H]⁺/426.0480 found 426.0478 [M - H]⁻.

***N*-((8-Fluoro-2-oxo-1,2-dihydroquinolin-4-yl)methyl)-*N*-((3-fluorophenyl)-4-methylthiazole-5-carboxamide (14)**. Compound **14** was synthesized as described for compound **7** using 4-((3-fluorophenylamino)methyl)-8-fluoroquinolin-2(1*H*)-one (**58**) and 4-methylthiazole-5-carboxylic acid as starting materials; HPLC: *t*_R = 5.95 (>98%); mp = 227.1 °C. ¹H NMR (400 MHz, DMSO-*d*₆) δ 11.78 (s, 1H), 8.92 (s, 1H), 7.66 (d, 1H, *J* = 8.4 Hz), 7.44 (m, 1H), 7.31–7.19 (m, 3H), 7.11 (m, 1H), 6.94 (d, 1H, *J* = 8.4 Hz), 6.42 (s, 1H), 5.34 (s, 2H), 2.42 (s, 3H). ¹³C NMR (400 MHz, DMSO-*d*₆) δ 162.8, 161.9 (d, *J* = 244 Hz, F coupling), 160.8, 155.8, 155.4, 149.0 (d, *J* = 244 Hz, F coupling), 145.3, 142.7 (d, *J* = 10.3 Hz), 130.8 (d, *J* = 9.5 Hz), 127.6 (d, *J* = 14.0 Hz), 124.0, 121.7 (d, *J* = 6.6 Hz), 121.4, 119.8, 119.6, 115.8 (d, *J* = 16.9 Hz), 114.9, 114.8, 114.7, 49.7, 16.7. LRMS (ESI⁺)/HRMS (ESI⁻) *m/z*: calcd for C₂₁H₁₅F₂N₃O₂S 412.1, found 412.2 [M + H]⁺/410.0775 found 410.0771 [M - H]⁻.

***N*-(3-Cyanophenyl)-*N*-((8-fluoro-2-oxo-1,2-dihydroquinolin-4-yl)methyl)-4-methylthiazole-5-carboxamide (15).** Compound 15 was synthesized as described for compound 7 using 8-fluoro-4-((3-cyanophenylamino)methyl)quinolin-2(1*H*)-one (59) and 4-methylthiazole-5-carboxylic acid as starting materials; HPLC: $t_R = 5.84$ (>98%); mp = 273.2 °C. $^1\text{H NMR}$ (400 MHz, DMSO- d_6) δ 11.76 (s, 1H), 8.93 (s, 1H), 7.98 (s, 1H), 7.71 (m, 1H), 7.64 (d, 1H, $J = 8.4$ Hz), 7.47–7.42 (m, 3H), 7.22 (m, 1H), 6.45 (s, 1H), 5.37 (s, 2H), 2.47 (s, 3H). LRMS (ESI+)/HRMS (ESI-) m/z : calcd for $\text{C}_{22}\text{H}_{15}\text{FN}_4\text{O}_2\text{S}$ 419.1, found 419.0 [M + H] $^+$ /417.0822 found 417.0821 [M - H] $^-$.

***N*-(3-Methylphenyl)-*N*-((8-fluoro-2-oxo-1,2-dihydroquinolin-4-yl)methyl)-4-methylthiazole-5-carboxamide (16).** Compound 16 was synthesized as described for compound 7 using 8-fluoro-4-((*m*-tolylamino)methyl)quinolin-2(1*H*)-one (60) and 4-methylthiazole-5-carboxylic acid as starting materials; HPLC: $t_R = 6.15$ (100%). $^1\text{H NMR}$ (400 MHz, DMSO- d_6) δ 11.75 (s, 1H), 8.89 (s, 1H), 7.67 (d, 1H, $J = 8.0$ Hz), 7.44 (dd, 1H, $J = 10.8, 8.4$ Hz), 7.23–7.12 (m, 2H), 7.06 (m, 2H), 6.88 (d, 1H, $J = 7.6$ Hz), 6.38 (s, 1H), 5.30 (s, 2H), 2.43 (s, 3H), 2.19 (s, 3H). LRMS (ESI+)/HRMS (ESI-) m/z : calcd for $\text{C}_{22}\text{H}_{18}\text{FN}_3\text{O}_2\text{S}$ 408.1, found 408.3 [M + H] $^+$ /406.1026 found 406.1027 [M - H] $^-$.

***N*-(3-Methoxyphenyl)-*N*-((8-fluoro-2-oxo-1,2-dihydroquinolin-4-yl)methyl)-4-methylthiazole-5-carboxamide (17).** Compound 17 was synthesized as described for compound 7 using 8-fluoro-4-((3-methoxyphenylamino)methyl)quinolin-2(1*H*)-one (61) and 4-methylthiazole-5-carboxylic acid as starting materials; HPLC: $t_R = 5.98$ (100%). $^1\text{H NMR}$ (400 MHz, DMSO- d_6) δ 11.75 (s, 1H), 8.90 (s, 1H), 7.68 (d, 1H, $J = 8.0$ Hz), 7.44 (ddd, 1H, $J = 10.0, 7.2, 0.8$ Hz), 7.24–7.13 (m, 2H), 6.80 (m, 2H), 6.63 (d, 1H, $J = 7.6$ Hz), 6.40 (s, 1H), 5.32 (s, 2H), 3.64 (s, 3H), 2.43 (s, 3H). $^{13}\text{C NMR}$ (400 MHz, DMSO- d_6) δ 162.8, 160.9, 159.6, 155.6, 155.2, 149.0 (d, $J = 245$ Hz, F coupling), 145.6, 142.1, 130.0, 127.6 (d, $J = 13.9$ Hz), 124.2, 121.6 (d, $J = 13.9$ Hz), 121.4, 120.0, 119.9 (d, $J = 3.0$ Hz), 119.7 (d, $J = 3.0$ Hz), 115.8 (d, $J = 17.6$ Hz), 113.5, 113.3, 55.2, 49.7, 16.7. LRMS (ESI+)/HRMS (ESI-) m/z : calcd for $\text{C}_{22}\text{H}_{18}\text{FN}_3\text{O}_3\text{S}$ 424.1, found 424.3 [M + H] $^+$ /422.0975 found 422.0974 [M - H] $^-$.

***N*-(3-Chlorophenyl)-*N*-((8-fluoro-2-oxo-1,2-dihydroquinolin-4-yl)methyl)thiazole-5-carboxamide (18).** Compound 18 was synthesized as described for compound 7 using 8-fluoro-4-((3-chlorophenylamino)methyl)quinolin-2(1*H*)-one (56) and thiazole-5-carboxylic acid as starting materials; HPLC: $t_R = 6.14$ (>97%); mp > 300 °C. $^1\text{H NMR}$ (400 MHz, DMSO- d_6) δ 11.75 (s, 1H), 9.10 (s, 1H), 7.66 (s, 1H), 7.62 (d, 1H, $J = 8.0$ Hz), 7.58 (t, 1H, $J = 2.0$ Hz), 7.48–7.37 (m, 3H), 7.24–7.16 (m, 2H), 6.47 (s, 1H), 5.30 (s, 2H). LRMS (ESI+)/HRMS (ESI-) m/z : calcd for $\text{C}_{20}\text{H}_{13}\text{ClFN}_3\text{O}_2\text{S}$ 414.0, found 414.2 [M + H] $^+$ /412.0323 found 412.0323 [M - H] $^-$.

***N*-(3-Chlorophenyl)-*N*-((8-fluoro-2-oxo-1,2-dihydroquinolin-4-yl)methyl)-2-methylnicotinamide (19).** Compound 19 was synthesized as described for compound 7 using 8-fluoro-4-((3-chlorophenylamino)methyl)quinolin-2(1*H*)-one (56) and 2-methylnicotinic acid as starting materials; HPLC: $t_R = 5.09$ (>98%); mp = 216.2 °C. $^1\text{H NMR}$ (400 MHz, DMSO- d_6 , TFA salt) δ 11.76 (s, 1H), 8.30 (d, 1H, $J = 3.6$ Hz), 7.72 (d, 1H, $J = 7.2$ Hz), 7.60 (d, 1H, $J = 7.6$ Hz), 7.45 (m, 1H), 7.39 (s, 1H), 7.26–7.21 (m, 1H), 7.18–7.11 (m, 2H), 7.06 (m, 1H), 6.92 (m, 1H), 6.46 (s, 1H), 5.38 (s, 2H), 2.43 (s, 3H). $^{13}\text{C NMR}$ (400 MHz, DMSO- d_6 , TFA salt) δ 168.5, 160.8, 153.7, 149.0 (d, $J = 245$ Hz, F coupling), 149.3, 145.2, 141.9, 135.1, 133.0, 130.9, 130.4, 127.7, 127.5, 127.4, 126.6, 122.4, 121.7 (d, $J = 6.6$ Hz), 120.3, 120.0, 119.6, 115.8 (d, $J = 16.8$ Hz), 48.6, 22.3. LRMS (ESI+)/HRMS (ESI-) m/z : calcd for $\text{C}_{23}\text{H}_{17}\text{ClFN}_3\text{O}_2$ 422.1, found 422.3 [M + H] $^+$ /420.0915 found 420.0919 [M - H] $^-$.

***N*-(3-Chlorophenyl)-*N*-((8-fluoro-2-oxo-1,2-dihydroquinolin-4-yl)methyl)-3-methylisonicotinamide (20).** Compound 20 was synthesized as described for compound 7 using 8-fluoro-4-((3-chlorophenylamino)methyl)quinolin-2(1*H*)-one (56) and 3-methylisonicotinic acid as starting materials; HPLC: $t_R = 5.07$ (>97%). $^1\text{H NMR}$ (400 MHz, MeOD, TFA salt) δ 8.63 (s, 1H), 8.50 (d, 1H, $J = 5.6$ Hz), 7.81 (d, 1H, $J = 8.4$ Hz), 7.76 (d, 1H, $J = 5.6$ Hz),

7.44 (m, 1H), 7.37 (m, 1H), 7.33 (m, 1H), 7.25 (m, 1H), 7.18 (m, 1H), 6.99 (d, 1H, $J = 8.0$ Hz), 6.58 (s, 1H), 5.49 (s, 2H), 2.52 (s, 3H). LRMS (ESI+)/HRMS (ESI-) m/z : calcd for $\text{C}_{23}\text{H}_{17}\text{ClFN}_3\text{O}_2$ 422.1, found 422.3 [M + H] $^+$ /420.0915 found 420.0915 [M - H] $^-$.

***N*-(3-Chlorophenyl)-*N*-((8-fluoro-2-oxo-1,2-dihydroquinolin-4-yl)methyl)-4-methylnicotinamide (21).** Compound 21 was synthesized as described for compound 7 using 8-fluoro-4-((3-chlorophenylamino)methyl)quinolin-2(1*H*)-one (56) and 4-methylnicotinic acid as starting materials; HPLC: $t_R = 5.21$ (>99%). $^1\text{H NMR}$ (400 MHz, DMSO- d_6 , TFA salt) δ 10.52 (s, 1H), 8.44 (d, 1H, $J = 5.2$ Hz), 8.34 (s, 1H), 8.27 (d, 1H, $J = 4.8$ Hz), 7.85 (d, 1H, $J = 7.6$ Hz), 7.42 (t, 1H, $J = 8.0$ Hz), 7.31–7.28 (m, 2H), 7.22–7.15 (m, 2H), 7.08 (m, 1H), 6.53 (s, 1H), 5.51 (s, 2H), 2.42 (s, 3H). LRMS (ESI+)/HRMS (ESI-) m/z : calcd for $\text{C}_{23}\text{H}_{17}\text{ClFN}_3\text{O}_2$ 422.1, found 422.3 [M + H] $^+$ /420.0915 found 420.0919 [M - H] $^-$.

***N*-(3-Chlorophenyl)-*N*-((8-fluoro-2-oxo-1,2-dihydroquinolin-4-yl)methyl)-3-methylpicolinamide (22).** Compound 22 was synthesized as described for compound 7 using 8-fluoro-4-((3-chlorophenylamino)methyl)quinolin-2(1*H*)-one (56) and 3-methylpicolinic acid as starting materials; HPLC: $t_R = 6.23$ (>93%). $^1\text{H NMR}$ (400 MHz, DMSO- d_6 , TFA salt) δ 11.77 (s, 1H), 8.20 (s, 1H), 7.70 (d, 1H, $J = 8.0$ Hz), 7.59 (d, 1H, $J = 6.8$ Hz), 7.46 (t, 1H, 8.0 Hz), 7.26–7.18 (m, 3H), 7.13 (m, 2H), 6.91 (s, 1H), 6.54 (s, 1H), 5.39 (s, 2H), 2.47 (s, 3H). $^{13}\text{C NMR}$ (400 MHz, DMSO- d_6 , TFA salt) δ 168.0, 160.9, 152.9, 149.0 (d, $J = 244$ Hz, F coupling), 145.9, 145.5, 145.4, 142.1, 138.3, 132.7, 130.5, 130.2, 127.0, 126.5, 125.6, 124.0, 121.7 (d, $J = 6.6$ Hz), 121.3, 119.9, 119.6, 115.9 (d, $J = 16.8$ Hz), 48.4, 17.2. LRMS (ESI+)/HRMS (ESI-) m/z : calcd for $\text{C}_{23}\text{H}_{17}\text{ClFN}_3\text{O}_2$ 422.1, found 422.1 [M + H] $^+$ /420.0915 found 420.0919 [M - H] $^-$.

***N*-(3-Chlorophenyl)-*N*-((8-fluoro-2-oxo-1,2-dihydroquinolin-4-yl)methyl)-1-methyl-1*H*-imidazole-5-carboxamide (23).** Sodium hydride (19 mg, 0.50 mmol) was added to a stirred solution of *N*-(3-chlorophenyl)-1-methyl-1*H*-imidazole-5-carboxamide (66, 100 mg, 0.42 mmol) in DMF (6 mL) at 25 °C. After 1 h, 2-(*tert*-butyldimethylsilyloxy)-8-fluoro-4-(iodomethyl)quinoline (63, 208 mg, 0.50 mmol) was added in one portion. The resulting mixture was stirred for 2.5 h, diluted with 1:1 hexanes:EtOAc (100 mL), washed with H₂O (50 mL), 5% aqueous sodium bicarbonate (50 mL), and brine, and then dried over MgSO₄, filtered, and concentrated under reduced pressure. The crude residue was purified by reversed-phase semipreparative HPLC (ACN:H₂O + 0.1% TFA) to afford *N*-(3-chlorophenyl)-*N*-((8-fluoro-2-oxo-1,2-dihydroquinolin-4-yl)methyl)-1-methyl-1*H*-imidazole-4-carboxamide (23, 29 mg, 17%) as a white solid. HPLC: $t_R = 4.88$ (>97%). $^1\text{H NMR}$ (400 MHz, DMSO- d_6) δ 11.74 (s, 1H), 7.70 (s, 1H), 7.63 (d, 1H, $J = 8.4$ Hz), 7.52 (s, 1H), 7.44 (m, 1H), 7.34 (m, 2H), 7.26–7.18 (m, 2H), 6.47 (s, 1H), 6.17 (s, 1H), 5.28 (s, 2H), 3.83 (s, 3H). LRMS (ESI+)/HRMS (ESI-) m/z : calcd for $\text{C}_{21}\text{H}_{16}\text{ClFN}_4\text{O}_2$ 411.1, found 411.2 [M + H] $^+$ /409.0868 found 409.0863 [M - H] $^-$.

***N*-(3-Chlorophenyl)-*N*-((8-fluoro-2-oxo-1,2-dihydroquinolin-4-yl)methyl)-3,5-dimethylisoxazole-4-carboxamide (24).** Compound 24 was synthesized as described for compound 7 using 8-fluoro-4-((3-chlorophenylamino)methyl)quinolin-2(1*H*)-one (56) and 3,5-dimethylisoxazole-4-carboxylic acid as starting materials; HPLC: $t_R = 6.30$ (100%); mp = 240.2 °C. $^1\text{H NMR}$ (400 MHz, DMSO- d_6) δ 11.75 (s, 1H), 7.65 (d, 1H, $J = 8.4$ Hz), 7.49 (m, 1H), 7.44 (m, 1H), 7.27–7.22 (m, 3H), 7.05 (m, 1H), 6.37 (s, 1H), 5.38 (s, 2H), 2.11 (s, 3H), 2.08 (s, 3H). $^{13}\text{C NMR}$ (DMSO- d_6) δ 167.9, 162.4, 160.8, 157.9, 149.0 (d, $J = 244$ Hz, F coupling), 145.2, 142.1, 133.1, 130.5, 127.6 (d, $J = 13.2$ Hz), 127.1, 126.4, 125.8, 121.6 (d, $J = 6.6$ Hz), 121.4, 119.8 (d, $J = 3.7$ Hz), 119.5 (d, $J = 3.0$ Hz), 115.8 (d, $J = 17.6$ Hz), 112.5, 48.9, 11.7, 10.2. LRMS (ESI+)/HRMS (ESI-) m/z : calcd for $\text{C}_{22}\text{H}_{17}\text{ClFN}_3\text{O}_3$ 426.1, found 426.3 [M + H] $^+$ /424.0864 found 424.0865 [M - H] $^-$.

***N*-(3-Chlorophenyl)-*N*-((8-fluoro-2-oxo-1,2-dihydroquinolin-4-yl)methyl)cyclopentanecarboxamide (25).** Compound 25 was synthesized as described for compound 7 using 8-fluoro-4-((3-chlorophenylamino)methyl)quinolin-2(1*H*)-one (56) and cyclopentanecarbonyl chloride (acid chloride commercially available) as starting materials; HPLC: $t_R = 6.94$ (>95%); mp = 188.4 °C. $^1\text{H NMR}$

(400 MHz, DMSO- d_6) δ 11.72 (s, 1H), 7.54 (d, 1H, J = 8.4 Hz), 7.43–7.38 (m, 4H), 7.19–7.11 (m, 2H), 6.28 (s, 1H), 5.09 (s, 2H), 2.59 (m, 1H), 1.70–1.36 (m, 8H). ^{13}C NMR (400 MHz, DMSO- d_6) δ 175.3, 160.9, 149.0 (d, J = 244 Hz, F coupling), 145.8, 142.9, 133.5, 131.0, 128.0, 127.6, 127.5, 127.1, 121.6, 121.5, 119.8 (d, J = 3.7 Hz), 119.7, 115.7 (d, J = 16.9 Hz), 49.3, 41.4, 30.5 (2C), 25.7 (2C). LRMS (ESI+)/HRMS (ESI-) m/z : calcd for $\text{C}_{22}\text{H}_{20}\text{ClFN}_2\text{O}_2$ 399.1, found 399.3 [M + H] $^+$ /397.1119 found 397.1122 [M - H] $^-$.

***N*-(3-Chlorophenyl)-*N*-((8-fluoro-2-oxo-1,2-dihydroquinolin-4-yl)methyl)isobutyramide (26).** Compound 26 was synthesized as described for compound 7 using 8-fluoro-4-((3-chlorophenylamino)methyl)quinolin-2(1*H*)-one (56) and isobutyryl chloride (acid chloride commercially available) as starting materials; HPLC: t_R = 6.45 (100%). ^1H NMR (400 MHz, DMSO- d_6) δ 11.72 (s, 1H), 7.53 (d, 1H, J = 7.6 Hz), 7.44–7.37 (m, 4H), 7.19–7.14 (m, 2H), 6.28 (s, 1H), 5.08 (s, 2H), 2.48 (m, 1H), 0.96 (d, 6H, J = 6.8 Hz). LRMS (ESI+)/HRMS (ESI-) m/z : calcd for $\text{C}_{20}\text{H}_{18}\text{ClFN}_2\text{O}_2$ 373.1, found 373.3 [M + H] $^+$ /371.0963 found 371.0957 [M - H] $^-$.

***N*-(3-Chlorophenyl)-4-methyl-*N*-((2-oxo-1,2-dihydropyridin-4-yl)methyl)thiazole-5-carboxamide (27).** *N*-(3-chlorophenyl)-*N*-((2-chloropyridin-4-yl)methyl)-4-methylthiazole-5-carboxamide (69, 400 mg, 0.91 mmol) in AcOH (40 mL) was heated to 140 °C for 2 days. The solvent was removed by evaporation under reduced pressure and the residue was purified by silica gel column chromatography (50:1 DCM/MeOH) to afford 200 mg (60%) of *N*-(3-chlorophenyl)-4-methyl-*N*-((2-oxo-1,2-dihydropyridin-4-yl)methyl)thiazole-5-carboxamide (27) as a yellow solid. HPLC: t_R = 5.28 (>98%); mp = 102.1 °C. ^1H NMR (400 MHz, DMSO- d_6) δ 11.47 (s, 1H), 8.92 (s, 1H), 7.40 (m, 1H), 7.32 (m, 3H), 7.10 (dt, 1H, J = 6.0, 2.4 Hz), 6.12 (s, 1H), 6.10 (s, 1H), 4.89 (s, 2H), 2.39 (s, 3H). ^{13}C NMR (400 MHz, DMSO- d_6) δ 162.8, 162.2, 155.6, 155.4, 150.5, 142.8, 135.4, 133.2, 130.7, 127.6, 127.3, 126.6, 124.1, 117.4, 104.3, 51.7, 16.7. LRMS (ESI+)/HRMS (ESI-) m/z : calcd for $\text{C}_{17}\text{H}_{14}\text{ClN}_3\text{O}_2\text{S}$ 360.0, found 360.2 [M + H] $^+$ /358.0417 found 358.0417 [M - H] $^-$.

***N*-(3-Chlorophenyl)-4-methyl-*N*-((2-oxo-1,2,5,6,7,8-hexahydroquinolin-4-yl)methyl)thiazole-5-carboxamide (28).** Compound 28 was synthesized as described for compound 27 using *N*-((2-chloro-5,6,7,8-tetrahydroquinolin-4-yl)methyl)-*N*-(3-chlorophenyl)-4-methylthiazole-5-carboxamide (74) as the starting material; HPLC: t_R = 6.16 (100%); mp = 223.4 °C. ^1H NMR (400 MHz, DMSO- d_6) δ 11.30 (s, 1H), 8.93 (s, 1H), 7.43 (s, 1H), 7.31 (m, 2H), 7.15 (m, 1H), 5.98 (s, 1H), 4.86 (s, 2H), 3.33 (m, 3H), 2.48–2.34 (m, 4H), 1.63 (m, 4H). ^{13}C NMR (DMSO- d_6) δ 162.6, 161.6, 155.7, 155.3, 149.6, 143.2, 142.7, 133.3, 130.7, 127.5, 127.0, 126.4, 124.1, 113.6, 110.3, 50.3, 26.5, 22.1, 21.9, 20.9, 16.6. LRMS (ESI+)/HRMS (ESI-) m/z : calcd for $\text{C}_{21}\text{H}_{20}\text{ClN}_3\text{O}_2\text{S}$ 414.1, found 414.3 [M + H] $^+$ /412.0887 found 412.0889 [M - H] $^-$.

***N*-(3-Chlorophenyl)-*N*-((8-fluoro-2-oxo-2*H*-chromen-4-yl)methyl)-5-methylthiazole-4-carboxamide (29).** Compound 29 was synthesized as described for compound 7 using 4-((3-chlorophenylamino)methyl)-8-fluoro-2*H*-chromen-2-one (79) and 4-methylthiazole-5-carboxylic acid as starting materials (propylamine step not necessary); HPLC: t_R = 6.83 (>99%); mp = 186.5 °C. ^1H NMR (400 MHz, DMSO- d_6) δ 8.95 (s, 1H), 7.70 (d, 1H, J = 8.4 Hz), 7.64 (m, 2H), 7.40 (m, 1H), 7.34 (m, 2H), 7.26 (d, 1H, J = 7.2 Hz), 6.50 (s, 1H), 5.37 (s, 2H), 2.44 (s, 3H). ^{13}C NMR (400 MHz, DMSO- d_6) δ 162.9, 158.1, 156.2, 155.6, 150.3, 148.7 (d, J = 247 Hz, F coupling), 142.6, 141.2 (d, J = 11.0 Hz), 133.4, 130.7, 127.9, 127.5, 126.7, 124.4 (d, J = 6.6 Hz), 123.7, 120.2, 119.5, 118.4 (d, J = 16.2 Hz), 113.9, 49.6, 16.8. LRMS (ESI+)/HRMS (ESI-) m/z : calcd for $\text{C}_{21}\text{H}_{14}\text{ClFN}_3\text{O}_3\text{S}$ 429.0, found 429.1 [M + H] $^+$ /427.0320 found 427.0321 [M - H] $^-$.

***N*-(3-Chlorophenyl)-*N*-((8-fluoro-2-methoxyquinolin-4-yl)methyl)-4-methylthiazole-5-carboxamide (30) and *N*-(3-chlorophenyl)-*N*-((8-fluoro-1-methyl-2-oxo-1,2-dihydroquinolin-4-yl)methyl)-4-methylthiazole-5-carboxamide (31).** Sodium hydride (60% in mineral oil, 5 mg, 0.12 mmol) was added to a suspension of *N*-(3-chlorophenyl)-*N*-((8-fluoro-2-oxo-1,2-dihydroquinolin-4-yl)methyl)-4-methylthiazole-5-carboxamide (12, 25 mg, 0.06 mmol) in DCM

(2 mL). Dimethylsulfate (6.6 μL , 0.07 mmol) was then added, and the resulting mixture was stirred at 25 °C for 18 h. The solvent was removed, and the residue was purified via reversed-phase semipreparative HPLC (ACN:H₂O+0.1% TFA) to afford 12 mg of *N*-(3-chlorophenyl)-*N*-((8-fluoro-1-methyl-2-oxo-1,2-dihydroquinolin-4-yl)methyl)-4-methylthiazole-5-carboxamide (31) as the first eluting isomer; HPLC: t_R = 6.74 (100%); ^1H NMR (400 MHz, DMSO- d_6) δ 8.94 (s, 1H), 7.74 (d, 1H, J = 8.4 Hz), 7.54 (t, 1H, J = 8.2 Hz), 7.49 (m, 1H), 7.35–7.26 (m, 3H), 7.10 (dt, 1H, J = 7.5, 2.0 Hz), 6.55 (s, 1H), 5.36 (s, 2H), 3.73 (d, 3H, J = 9.2 Hz), 2.43 (s, 3H); LRMS (ESI+)/HRMS (ESI+) m/z : calcd for $\text{C}_{22}\text{H}_{17}\text{ClFN}_3\text{O}_2\text{S}$ 442.1, found 442.3 [M + H] $^+$ /442.0792 found 442.0789 [M + H] $^+$; and 10 mg of *N*-(3-chlorophenyl)-*N*-((8-fluoro-2-methoxyquinolin-4-yl)methyl)-4-methylthiazole-5-carboxamide (30) as the second eluting isomer; HPLC: t_R = 7.38 (>99%); mp = 150.5 °C; ^1H NMR (400 MHz, DMSO- d_6) δ 8.92 (s, 1H), 7.87 (d, 1H, J = 8.0 Hz), 7.56–7.43 (m, 3H), 7.28 (m, 1H), 7.22 (t, 1H, J = 8.0 Hz), 7.05 (dt, 1H, J = 7.6, 1.6 Hz), 6.95 (s, 1H), 5.55 (s, 2H), 3.95 (s, 3H), 2.43 (s, 3H); ^{13}C NMR (400 MHz, DMSO- d_6) δ 162.8, 161.7, 156.3 (d, J = 251 Hz, F coupling), 155.8, 155.4, 145.4, 142.5, 135.7 (d, J = 11.7 Hz), 133.3, 130.6, 127.8, 127.4, 126.7, 124.9, 124.1 (d, J = 7.3 Hz), 124.0, 119.3 (d, J = 4.4 Hz), 114.5 (d, J = 19.0 Hz), 112.5, 53.3, 49.6, 16.7; LRMS (ESI+)/HRMS (ESI-) m/z : calcd for $\text{C}_{22}\text{H}_{17}\text{ClFN}_3\text{O}_2\text{S}$ 442.1, found 442.3 [M + H] $^+$ /440.0636 found 440.0640 [M - H] $^-$.

***N*-(3-Chlorophenyl)-*N*-((8-fluoroquinolin-4-yl)methyl)-4-methylthiazole-5-carboxamide (32).** Compound 32 was synthesized as described for compound 7 using 3-chloro-*N*-((8-fluoroquinolin-4-yl)methyl)benzenamine (82) and 4-methylthiazole-5-carboxylic acid as starting materials (propylamine step not necessary); HPLC: t_R = 6.18 (>98%); mp = 175.3 °C. ^1H NMR (400 MHz, DMSO- d_6) δ 8.93 (s, 1H), 8.86 (d, 1H, J = 4.4 Hz), 8.00 (dd, 1H, J = 8.0, 1.6 Hz), 7.68–7.58 (m, 2H), 7.54 (d, 1H, J = 4.4 Hz), 7.50 (t, 1H, J = 2.0 Hz), 7.27 (m, 1H), 7.22 (t, 1H, J = 8.0 Hz), 7.10 (d, 1H, J = 7.6 Hz), 5.63 (s, 2H), 2.44 (s, 3H). ^{13}C NMR (400 MHz, DMSO- d_6) δ 162.8, 157.6 (d, J = 254 Hz, F coupling), 155.8, 155.4, 150.4, 142.6, 142.0 (d, J = 2.9 Hz), 137.6 (d, J = 11.7 Hz), 133.2, 130.6, 127.8, 127.7, 127.6 (d, J = 2.5 Hz), 126.9 (d, J = 4.4 Hz), 126.8, 123.9, 121.1, 119.5 (d, J = 5.2 Hz), 113.6 (d, J = 18.3 Hz), 49.8, 16.7. LRMS (ESI+)/HRMS (ESI-) m/z : calcd for $\text{C}_{21}\text{H}_{15}\text{ClFN}_3\text{OS}$ 412.1, found 412.2 [M + H] $^+$ /410.0530 found 410.0533 [M - H] $^-$.

***N*-(3-Chlorophenyl)-*N*-((8-fluoroisquinolin-4-yl)methyl)-4-methylthiazole-5-carboxamide (33).** Compound 33 was synthesized as described for compound 7 using 3-chloro-*N*-((8-fluoroisquinolin-4-yl)methyl)benzenamine (91) and 4-methylthiazole-5-carboxylic acid as starting materials (propylamine step not necessary); HPLC: t_R = 5.59 (>98%); mp = 100 °C (decomposition). ^1H NMR (400 MHz, DMSO- d_6 , HCl salt) δ 9.62 (s, 1H), 8.90 (s, 1H), 8.51 (s, 1H), 8.15–8.07 (m, 2H), 7.72 (ddd, 1H, J = 10.8, 7.6, 1.2 Hz), 7.47 (t, 1H, J = 2.0 Hz), 7.25 (m, 1H), 7.16 (t, 1H, J = 8.0 Hz), 6.91 (d, 1H, J = 8.0 Hz), 5.66 (s, 2H), 2.43 (s, 3H). ^{13}C NMR (400 MHz, DMSO- d_6 , HCl salt) δ 162.9, 159.3 (d, J = 258 Hz, F coupling), 155.8, 155.6, 143.1 (d, J = 5.1 Hz), 141.9, 136.6, 136.3 (d, J = 9.6 Hz), 135.8, 133.3, 130.7, 129.8, 128.2, 127.2, 123.8, 119.9 (d, J = 4.4 Hz), 118.0 (d, J = 15.4 Hz), 113.9 (d, J = 17.6 Hz), 54.9, 47.3, 16.8. LRMS (ESI+)/HRMS (ESI+) m/z : calcd for $\text{C}_{21}\text{H}_{15}\text{ClFN}_3\text{OS}$ 412.1, found 412.2 [M + H] $^+$ /412.0686 found 412.0682 [M + H] $^+$.

4-((*N*-(3-Chlorophenyl)-4-methylthiazole-5-carboxamido)methyl)-8-fluoroisquinoline 2-Oxide (34). A mixture of *N*-(3-chlorophenyl)-*N*-((8-fluoroisquinolin-4-yl)methyl)-4-methylthiazole-5-carboxamide (33, 124 mg, 302 μmol) and *m*-CPBA (156 mg, 905 μmol) in DCM (10 mL) was stirred at 25 °C for 1 h. The solvent was removed under reduced pressure, and the residue was purified by silica gel column chromatography (0 to 10% MeOH/DCM) to afford 80 mg (62%) of 4-((*N*-(3-chlorophenyl)-4-methylthiazole-5-carboxamido)methyl)-8-fluoroisquinoline 2-oxide (34) as an off-white solid; HPLC: t_R = 6.05 (>99%); mp = 171.4 °C. ^1H NMR (400 MHz, DMSO- d_6) δ 8.91 (s, 1H), 8.78 (s, 1H), 8.10 (s, 1H), 7.94 (d, 1H, J = 8.4 Hz), 7.70 (m, 1H), 7.55 (m, 1H), 7.44 (s, 1H), 7.32 (m, 1H), 7.21 (t, 1H, J = 8.0 Hz), 6.92 (d, 1H, J = 8.0 Hz), 5.54

(s, 2H), 2.44 (s, 3H). ^{13}C NMR (400 MHz, DMSO- d_6) δ 162.8, 156.7, 155.5, 155.4 (d, $J = 252$ Hz, F coupling), 141.7, 138.0, 133.3, 131.1, 130.6, 129.2 (d, $J = 8.1$ Hz), 128.6 (d, $J = 4.4$ Hz), 128.1, 127.9, 127.7, 127.1, 123.8, 119.9 (d, $J = 17.9$ Hz), 119.5 (d, $J = 3.6$ Hz), 113.7 (d, $J = 18.3$ Hz), 46.7, 16.7. LRMS (ESI+)/HRMS (ESI-) m/z : calcd for $\text{C}_{21}\text{H}_{15}\text{ClFN}_3\text{O}_2\text{S}$ 428.1, found 428.2 [M + H] $^+$ /426.0480 found 426.0486 [M - H] $^-$.

***N*-(3-Chlorophenyl)-4-methyl-*N*-(2-oxo-1,2-dihydroquinolin-4-yl)methylthiazole-5-carboxamide (35).** Compound **35** was synthesized as described for compound **7** using 4-((3-chlorophenylamino)methyl)quinolin-2(1*H*)-one (**115**) and 4-methylthiazole-5-carboxylic acid as starting materials; HPLC: $t_{\text{R}} = 6.50$ (>98%). ^1H NMR (400 MHz, DMSO- d_6) δ 11.73 (s, 1H), 8.93 (s, 1H), 7.82 (d, 1H, $J = 7.6$ Hz), 7.50 (m, 1H), 7.43 (s, 1H), 7.32–7.22 (m, 4H), 7.05 (m, 1H), 6.34 (s, 1H), 5.35 (s, 2H), 2.42 (s, 3H). LRMS (ESI+)/HRMS (ESI-) m/z : calcd for $\text{C}_{21}\text{H}_{16}\text{ClN}_3\text{O}_2\text{S}$ 410.1, found 410.4 [M + H] $^+$ /408.0574 found 408.0568 [M - H] $^-$.

***N*-(8-Chloro-2-oxo-1,2-dihydroquinolin-4-yl)methyl-*N*-(3-chlorophenyl)-4-methylthiazole-5-carboxamide (36).** Compound **36** was synthesized as described for compound **7** using 8-chloro-4-((3-chlorophenylamino)methyl)quinolin-2(1*H*)-one (**116**) and 4-methylthiazole-5-carboxylic acid as starting materials; HPLC: $t_{\text{R}} = 6.57$ (>97%); mp = 211.4 °C. ^1H NMR (400 MHz, DMSO- d_6) δ 10.98 (s, 1H), 8.92 (s, 1H), 7.83 (d, 1H, $J = 7.6$ Hz), 7.69 (d, 1H, $J = 7.6$ Hz), 7.47 (s, 1H), 7.32–7.23 (m, 3H), 7.08 (dd, 1H, $J = 7.6$, 1.6 Hz), 6.45 (s, 1H), 5.36 (s, 2H), 2.42 (s, 3H). ^{13}C NMR (400 MHz, DMSO- d_6) δ 162.8, 161.0, 155.8, 155.5, 145.7, 142.5, 135.2, 133.3, 130.9, 130.7, 127.8, 127.4, 126.7, 123.9, 123.3, 122.4, 121.1, 119.3, 119.0, 49.7, 16.7. LRMS (ESI+)/HRMS (ESI-) m/z : calcd for $\text{C}_{21}\text{H}_{15}\text{Cl}_2\text{N}_3\text{O}_2\text{S}$ 444.0, found 444.2 [M + H] $^+$ /442.0184 found 442.0186 [M - H] $^-$.

***N*-(3-Chlorophenyl)-*N*-((7-fluoro-2-oxo-1,2-dihydroquinolin-4-yl)methyl)-4-methylthiazole-5-carboxamide (37).** Compound **37** was synthesized as described for compound **7** using 4-((3-chlorophenylamino)methyl)-7-fluoroquinolin-2(1*H*)-one (**117**) and 4-methylthiazole-5-carboxylic acid as starting materials; HPLC: $t_{\text{R}} = 6.79$ (100%); mp = 258.8 °C. ^1H NMR (400 MHz, DMSO- d_6) δ 11.83 (s, 1H), 8.94 (s, 1H), 7.90 (m, 1H), 7.46 (s, 1H), 7.30 (m, 2H), 7.13–7.06 (m, 3H), 6.36 (s, 1H), 5.35 (s, 2H), 2.44 (s, 3H). ^{13}C NMR (400 MHz, DMSO- d_6) δ 163.0 (d, $J = 246$ Hz, F coupling), 162.8, 161.3, 155.8, 155.4, 145.3, 142.5, 140.5 (d, $J = 11.7$ Hz), 133.3, 130.7, 127.8, 127.4, 126.7, 126.6, 123.9, 119.3, 114.5, 109.9 (d, $J = 23.4$ Hz), 101.5 (d, $J = 24.9$ Hz), 49.6, 16.7. LRMS (ESI+)/HRMS (ESI-) m/z : calcd for $\text{C}_{21}\text{H}_{15}\text{ClFN}_3\text{O}_2\text{S}$ 428.1, found 428.5 [M + H] $^+$ /426.0480 found 426.0482 [M - H] $^-$.

***N*-(3-Chlorophenyl)-*N*-((6-fluoro-2-oxo-1,2-dihydroquinolin-4-yl)methyl)-4-methylthiazole-5-carboxamide (38).** Compound **38** was synthesized as described for compound **7** using 4-((3-chlorophenylamino)methyl)-6-fluoroquinolin-2(1*H*)-one (**118**) and 4-methylthiazole-5-carboxylic acid as starting materials. HPLC: $t_{\text{R}} = 6.73$ (>99%); mp = 256.6 °C. ^1H NMR (400 MHz, DMSO- d_6) δ 11.85 (s, 1H), 8.95 (s, 1H), 7.68 (dd, 1H, $J = 10.0$, 2.8 Hz), 7.47–7.41 (m, 2H), 7.34–7.30 (m, 3H), 7.26 (t, 1H, $J = 8.0$ Hz), 7.04 (m, 1H), 6.41 (s, 1H), 5.38 (s, 1H), 2.40 (s, 3H). ^{13}C NMR (400 MHz, DMSO- d_6) δ 162.8, 160.8, 157.0 (d, $J = 237$ Hz, F coupling), 155.8, 155.5, 144.9, 142.4, 135.5, 133.3, 130.7, 127.8, 127.3, 126.7, 123.9, 121.5, 118.7 (d, $J = 24$ Hz), 118.1 (d, $J = 8.8$ Hz), 117.4 (d, $J = 8.8$ Hz), 109.5 (d, $J = 24$ Hz), 49.4, 16.6. LRMS (ESI+)/HRMS (ESI-) m/z : calcd for $\text{C}_{21}\text{H}_{15}\text{ClFN}_3\text{O}_2\text{S}$ 428.1, found 428.5 [M + H] $^+$ /426.0480 found 426.0472 [M - H] $^-$.

***N*-(3-Chlorophenyl)-*N*-((5-fluoro-2-oxo-1,2-dihydroquinolin-4-yl)methyl)-4-methylthiazole-5-carboxamide (39).** A mixture of *N*-((8-bromo-5-fluoro-2-oxo-1,2-dihydroquinolin-4-yl)methyl)-*N*-(3-chlorophenyl)-4-methylthiazole-5-carboxamide (**122**, 80 mg, 0.36 mmol) and Pd/C (cat.) in MeOH (5 mL) was hydrogenated for 18 h (with a balloon of hydrogen). The Pd/C was removed by filtration through celite, and the solvent was removed under reduced pressure. The residue was purified by semipreparative HPLC (ACN/water + 0.1% TFA) to afford 5.5 mg (3%) of *N*-(3-chlorophenyl)-*N*-((5-fluoro-2-oxo-1,2-dihydroquinolin-4-yl)methyl)-4-methylthiazole-5-carboxamide (**39**) as a white solid; HPLC: $t_{\text{R}} = 6.85$ (>97%). ^1H

NMR (DMSO- d_6) δ 11.99 (s, 1H), 8.97 (s, 1H), 7.54–7.51 (m, 2H), 7.33 (m, 2H), 7.25 (m, 1H), 7.16 (d, 1H, $J = 8.4$ Hz), 7.04 (d, 1H), 6.44 (s, 1H), 5.35 (s, 2H), 2.44 (s, 3H). LRMS (ESI+)/HRMS (ESI-) m/z : calcd for $\text{C}_{21}\text{H}_{15}\text{ClFN}_3\text{O}_2\text{S}$ 428.1, found 428.5 [M + H] $^+$ /426.0480 found 426.0487 [M - H] $^-$.

***N*-(3-Chlorophenyl)-*N*-((7,8-difluoro-2-oxo-1,2-dihydroquinolin-4-yl)methyl)-4-methylthiazole-5-carboxamide (40).** Compound **40** was synthesized as described for compound **7** using 4-((3-chlorophenylamino)methyl)-7,8-difluoroquinolin-2(1*H*)-one (**120**) and 4-methylthiazole-5-carboxylic acid as starting materials; HPLC: $t_{\text{R}} = 6.73$ (>96%); mp = 174.2 °C. ^1H NMR (DMSO- d_6) δ 12.03 (s, 1H), 8.95 (s, 1H), 7.70 (m, 1H), 7.49 (s, 1H), 7.37–7.28 (m, 3H), 7.09 (d, 1H, $J = 8.2$ Hz), 6.39 (s, 1H), 5.35 (s, 2H), 2.43 (s, 3H). ^{13}C NMR (400 MHz, DMSO- d_6) δ 162.8, 161.0, 155.9, 155.5, 150.0 (dd, $J = 247$, 9.2 Hz, F coupling), 145.2, 142.5, 136.9 (dd, $J = 240$, 9.2 Hz, F coupling), 133.3, 130.7, 129.6 (d, $J = 6.6$ Hz), 127.9, 127.4, 126.7, 123.9, 120.4, 120.2, 115.7, 110.3 (d, $J = 19.0$ Hz), 49.6, 16.7. LRMS (ESI+)/HRMS (ESI-) m/z : calcd for $\text{C}_{21}\text{H}_{14}\text{ClF}_2\text{N}_3\text{O}_2\text{S}$ 446.0, found 446.5 [M + H] $^+$ /444.0385 found 444.0381 [M - H] $^-$.

***N*-(3-Chlorophenyl)-*N*-((7,8-difluoro-2-oxo-1,2-dihydroquinolin-4-yl)methyl)-4-methylnicotinamide (41).** Compound **41** was synthesized as described for compound **7** using 4-((3-chlorophenylamino)methyl)-7,8-difluoroquinolin-2(1*H*)-one (**120**) and 4-methylnicotinic acid as starting materials; HPLC: $t_{\text{R}} = 5.29$ (>99%); mp = 187.7 °C. ^1H NMR (400 MHz, DMSO- d_6 , TFA salt) δ NH resonance not observed, 8.48 (s, 1H), 8.36 (d, 1H, $J = 4.8$ Hz), 7.73 (m, 1H), 7.47 (s, 1H), 7.33 (m, 2H), 7.20–7.12 (m, 2H), 6.95 (m, 1H), 6.44 (s, 1H), 5.37 (s, 2H), 2.35 (s, 3H). ^{13}C NMR (400 MHz, DMSO- d_6 , TFA salt) δ 166.8, 161.0, 150.1 (dd, $J = 247$, 9.5 Hz, F coupling), 147.5, 146.7, 145.7, 144.9, 141.6, 137.0 (dd, $J = 240$, 9.5 Hz, F coupling), 133.2, 132.5, 130.6, 129.5 (d, $J = 6.6$ Hz), 127.8, 127.5, 126.7, 126.0, 121.3, 120.6, 115.8, 110.4 (d, $J = 18.3$ Hz), 48.7, 18.8. LRMS (ESI+)/HRMS (ESI-) m/z : calcd for $\text{C}_{23}\text{H}_{16}\text{ClF}_2\text{N}_3\text{O}_2$ 440.1, found 440.3 [M + H] $^+$ /438.0821 found 438.0820 [M - H] $^-$.

***N*-(3-Chlorophenyl)-*N*-((7,8-difluoro-2-oxo-1,2-dihydroquinolin-4-yl)methyl)-1-methyl-1*H*-imidazole-5-carboxamide (42).** Compound **42** was synthesized as described for compound **23** using 4-(bromomethyl)-7,8-difluoroquinolin-2(1*H*)-one (**113**) as the starting material; HPLC: $t_{\text{R}} = 5.86$ (>97%). ^1H NMR (400 MHz, DMSO- d_6 , TFA salt) δ NH resonance not observed, 8.54 (s, 1H), 7.63 (m, 2H), 7.39–7.27 (m, 4H), 6.67 (s, 1H), 6.49 (s, 1H), 5.29 (s, 2H), 3.93 (s, 3H). ^{13}C NMR (400 MHz, DMSO- d_6 , TFA salt) δ 161.2, 160.5, 150.1 (dd, $J = 247$, 9.5 Hz, F coupling), 145.6, 143.8, 141.6, 137.0 (dd, $J = 240$, 15.4 Hz, F coupling), 134.2, 133.4, 130.8, 127.7, 127.5, 126.6, 124.9, 120.6, 118.8, 115.8, 115.7, 110.4 (d, $J = 19.0$ Hz), 49.6, 33.7. LRMS (ESI+)/HRMS (ESI-) m/z : calcd for $\text{C}_{21}\text{H}_{15}\text{ClF}_2\text{N}_4\text{O}_2$ 429.1, found 428.9 [M + H] $^+$ /427.0774 found 427.0773 [M - H] $^-$.

***N*-(3-Chlorophenyl)-*N*-((7,8-difluoro-2-oxo-1,2-dihydroquinolin-4-yl)methyl)-3,5-dimethylisoxazole-4-carboxamide (43).** Compound **43** was synthesized as described for compound **7** using 4-((3-chlorophenylamino)methyl)-7,8-difluoroquinolin-2(1*H*)-one (**120**) and 3,5-dimethylisoxazole-4-carboxylic acid as starting materials; HPLC: $t_{\text{R}} = 6.42$ (>95%). ^1H NMR (400 MHz, DMSO- d_6) δ 12.00 (s, 1H), 7.68 (m, 1H), 7.50 (s, 1H), 7.40–7.22 (m, 3H), 7.04 (m, 1H), 6.32 (s, 1H), 5.37 (s, 2H), 2.11 (s, 3H), 2.07 (s, 3H). LRMS (ESI+)/HRMS (ESI-) m/z : calcd for $\text{C}_{22}\text{H}_{16}\text{ClF}_2\text{N}_3\text{O}_3$ 444.1, found 444.3 [M + H] $^+$ /442.0770 found 442.0767 [M - H] $^-$.

***N*-(3-Chlorophenyl)-*N*-((3,8-difluoro-2-oxo-1,2-dihydroquinolin-4-yl)methyl)-4-methylthiazole-5-carboxamide (44).** Compound **44** was synthesized as described for compound **7** using 4-((3-chlorophenylamino)methyl)-3,8-difluoroquinolin-2(1*H*)-one (**121**) and 4-methylthiazole-5-carboxylic acid as starting materials. HPLC: $t_{\text{R}} = 6.19$ (>99%). ^1H NMR (400 MHz, DMSO- d_6) δ 12.38 (s, 1H), 8.88 (s, 1H), 7.80 (d, 1H, $J = 8.0$ Hz), 7.47 (t, 1H, $J = 10.8$ Hz), 7.38–7.30 (m, 3H), 7.19 (t, 1H, $J = 8.0$ Hz), 6.77 (d, 1H, $J = 7.6$ Hz), 5.44 (s, 2H), 2.42 (s, 3H). LRMS (ESI+)/HRMS (ESI-) m/z : calcd for $\text{C}_{21}\text{H}_{14}\text{ClF}_2\text{N}_3\text{O}_2\text{S}$ 446.0, found 446.2 [M + H] $^+$ /444.0385 found 444.0380 [M - H] $^-$.

Table 7. Mouse Pharmacokinetics of Compounds **12** and **42**

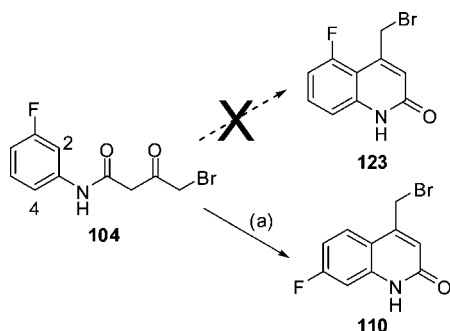
compd	C_{\max} (μM)	T_{\max} (h)	$t_{1/2}$ (h) ^c	AUC ($\mu\text{g}\cdot\text{h}/\text{mL}$)	Cl_p (mL/min/kg)	V_{dss} (L/kg)
12 ^a	1.4	0.5	0.9	0.45	>100	1.6
42 ^b	2.2	0.25	1.1	0.52	>100	1.1

^a 1 mg/kg iv; 10 mg/kg po. ^b 3 mg/kg iv; 10 mg/kg po. ^c po $t_{1/2}$.

Table 8. Cytochrome P450 Inhibition Values of Selected Compounds

compd	cytochrome P450 inhibition EC_{50} (μM)				
	CYP1A2	CYP3A4	CYP2D6	CYP2C9	CYP2C19
12	>100 ^a	7.0	>100 ^a	33	13
42	95	1.4	21	25	11
41	>100 ^a	3.4	>100 ^a	ND ^b	30
40	52	4.9	>100 ^a	22	19
26	>100 ^a	7.6	>100 ^a	ND ^b	42
47	>100 ^a	1.8	>100 ^a	55	93

^a <50% inhibition @100 μM . ^b Not determined.

Scheme 9^a

^a Reagents and conditions: (a) H_2SO_4 , 45 °C, 18 h.

***N*-(3-Chlorophenyl)-*N*-((7,8-difluoro-2-oxo-2H-chromen-4-yl)methyl)-4-methylthiazole-5-carboxamide (**45**).** Compound **45** was synthesized as described for compound **29** using 1-(3,4-difluoro-2-hydroxyphenyl)ethanone²⁹ as the starting material; HPLC: t_R = 7.02 (100%); mp = 170 °C. ¹H NMR (400 MHz, $\text{DMSO}-d_6$) δ 9.95 (s, 1H), 7.74 (m, 1H), 7.62 (m, 1H), 7.54 (m, 1H), 7.36–7.25 (m, 3H), 6.46 (s, 1H), 5.35 (s, 2H), 2.44 (s, 3H). ¹³C NMR (400 MHz, $\text{DMSO}-d_6$) δ 163.0, 157.9, 156.3, 155.6, 151.3 (dd, J = 250, 9.5 Hz, F coupling), 150.2, 142.7, 142.5, 137.5 (dd, J = 249, 15.4 Hz, F coupling), 133.4, 130.8, 127.9, 127.5, 126.8, 123.6, 120.3, 115.7 (d, J = 3.0 Hz), 112.7 (d, J = 13.2 Hz), 112.6 (d, J = 5.1 Hz), 49.5, 16.8. LRMS (ESI+)/HRMS (ESI-) m/z : calcd for $\text{C}_{21}\text{H}_{13}\text{ClF}_2\text{N}_2\text{O}_5\text{S}$ 447.0, found 447.2 [M + H]⁺/445.0225 found 445.0220 [M – H]⁻.

***N*-(3-Chlorophenyl)-*N*-((7,8-difluoroisoquinolin-4-yl)methyl)-4-methylthiazole-5-carboxamide (**46**).** Compound **46** was synthesized as described for compound **33** using 2,3-difluoro-6-iodobenzoic acid as the starting material; HPLC: t_R = 6.20 (>95%). ¹H NMR (400 MHz, $\text{DMSO}-d_6$) δ 9.57 (s, 1H), 8.91 (s, 1H), 8.45 (s, 1H), 8.19 (m, 2H), 7.42 (t, 1H, J = 2.4 Hz), 7.25 (d, 1H, J = 8.0 Hz), 7.16 (t, 1H, J = 8.0 Hz), 6.87 (d, 1H, J = 8.0 Hz), 5.64 (s, 2H), 2.42 (s, 3H). ¹³C NMR (400 MHz, $\text{DMSO}-d_6$) δ 162.7, 155.7, 155.5, 146.5 (dd, J = 248, 10.2 Hz, F coupling), 144.9 (dd, J = 255, 10.0 Hz, F coupling), 144.2, 141.8, 140.0, 133.3, 131.9, 130.6, 128.1 (d, J = 2.2 Hz), 127.6, 127.2, 124.4, 124.2, 123.9, 121.3, 119.2 (d, J = 10.9 Hz), 47.2, 16.7. LRMS (ESI+)/HRMS (ESI+) m/z : calcd for $\text{C}_{21}\text{H}_{14}\text{ClF}_2\text{N}_3\text{OS}$ 430.0, found 430.2 [M + H]⁺/430.0592 found 430.0585 [M + H]⁺.

4-((*N*-(3-Chlorophenyl)-4-methylthiazole-5-carboxamido)methyl)-7,8-difluoroisoquinoline 2-Oxide (47**).** Compound **47** was synthesized as described for compound **34** using *N*-(3-chlorophenyl)-*N*-((7,8-difluoroisoquinolin-4-yl)methyl)-4-methylthiazole-5-carboxamide (**46**) as the starting material; HPLC: t_R = 6.20 (>99%). ¹H NMR (400 MHz, $\text{DMSO}-d_6$) δ 8.89 (s, 1H), 8.82 (s, 1H), 8.06 (s, 1H), 7.97 (m, 1H), 7.88–7.81 (m, 1H), 7.45 (m, 1H), 7.29 (m, 1H), 7.21 (t, 1H, J = 8.0 Hz), 6.91 (d, 1H, J = 8.0 Hz), 5.51 (s,

2H), 2.42 (s, 3H). LRMS (ESI+)/HRMS (ESI-) m/z : calcd for $\text{C}_{21}\text{H}_{14}\text{ClF}_2\text{N}_3\text{O}_2\text{S}$ 446.0, found 446.2 [M + H]⁺/444.0385 found 444.0382 [M – H]⁻.

Biological Methods. Recombinant iNOS Assay (293 Transient Transfection Assay). HEK293 cells (ATCC) were seeded into 150 mm \times 25 mm tissue culture plates and grown to approximately 70% confluence in DMEM containing 10% FBS, 100 U/mL penicillin, and 100 $\mu\text{g}/\text{mL}$ streptomycin. Each plate was transfected with 1 mL of DMEM with Pen/Strep containing 10 μg of human or murine iNOS expression plasmid and 30 μL of Fugene 6 and incubated for 4 h at 37 °C and 10% CO_2 . Cells were trypsinized, resuspended to 5×10^5 cells/mL, and plated in 1536-well plates, followed by immediate treatment with compound. 1400W (100 μM final) was added as a positive control. After 18 h of incubation, NO production was measured by adding 2,3-diaminonaphthalene (DAN) at 10 $\mu\text{g}/\text{mL}$ final concentration (Invitrogen) diluted in DMEM supplemented with hydrochloric acid (0.1 N final) and incubated for 20 min at room temperature. Fluorescence was measured after increasing pH with sodium hydroxide (0.12 N final).³⁰

Recombinant eNOS and nNOS Assay (293 Transient Transfection Assays). HEK293 cells (ATCC) were seeded into 150 mm \times 25 mm tissue culture plates and grown to approximately 70% confluence in DMEM containing 10% FBS, 100 U/mL penicillin, and 100 $\mu\text{g}/\text{mL}$ streptomycin. Each plate was transfected with 1 mL DMEM with Pen/Strep containing 10 μg of human or murine eNOS or 15 μg of human eNOS expression plasmid along with Fugene 6 (added in a 3:1 ratio of μL Fugene to μg plasmid) and incubated for 4 h at 37 °C and 10% CO_2 . Cells were trypsinized, resuspended to 5×10^5 cells/mL, and plated in 384-well plates, followed by immediate treatment with compound. SEITU (100 μM final) was added as a positive control. Cells were incubated at 37 °C with 10% CO_2 for 24 h and then activated by calcium ionophore addition of either A23187 (83 nM final) for eNOS or ionomycin (30 μM final) for nNOS. After 18 h of incubation, NO production was measured as described for recombinant iNOS assay (above).

LPS Assay. A dose of 10 mg/kg of LPS (Sigma) was used in mouse endotoxemia studies. LPS was dissolved in 0.9% sodium chloride and was given as an intraperitoneal injection at volume of 10 mL/kg. Male mice (Balb/c) were returned to their home cages after injection and sacrificed 6 h later. Test compounds were administered by oral gavage (prepared in 90% PEG/5% Tween 80/5% PVP + 90% CMC (0.5% w/v)) immediately before LPS injection. Blood samples were collected into EDTA containing tubes and processed for plasma collection for analysis of nitrate and drug levels. Plasma nitrate (marker of iNOS activity) levels increase gradually with peak induction achieved 6–8 h postinjection. Prior to starting the reactions, plasma samples were subjected to filtration through a 10 kDa molecular weight cutoff filter (Fisher Scientific) at 2500 rpm. Nitrates were converted to nitrites using nitrate reductase, and then diaminonaphthalene (DAN) was added, followed by the addition of NaOH, which converts the nitrite–DAN adduct into a fluorophore. Measurement of the fluorescence of the nitrite–DAN adduct using an Aquest plate reader (Molecular Devices) accurately determines NO_2 concentration.

Mouse Formalin Pain Model. The formalin solution for intraplantar injection was first prepared by diluting a 10% formalin solution to 5% with 0.9% saline. Test compounds were administered by oral gavage (prepared in 90% PEG/5% Tween 80/5% PVP + 90% CMC (0.5% w/v)) 30 min prior to formalin injection. A volume of 20 μL of formalin solution was injected into the left hind paw of each animal. Immediately after injection of formalin into the left hind paw, the mouse was placed in a see-through observation chamber and a timer was activated. The duration of pain behaviors

(hind paw flinches, licking, and biting) displayed was counted in 5 min intervals. Phase II was observed from 25–45 min postformalin injection. Side effects observed were also noted. Data are presented as time spent in nociceptive behaviors during phase II (25–45 min postformalin). There was a single observer throughout the study. All results are expressed as mean \pm SE ($n = 5-6$ mice). Statistical significance is inferred from one way analysis of variance (ANOVA), followed by appropriate post hoc analyses (GraphPad Prism, V5.0).

Mouse Chronic Constriction Injury (CCI) Model. Mice underwent a surgical procedure previously described by Bennett and Xie. Briefly, mice were initially anesthetized with 5% isoflurane in medical grade pure oxygen and maintained at 2–3% isoflurane during the surgical procedure. Using aseptic techniques, the left sciatic nerve at the level of the mid thigh was exposed and loosely ligated with four ligatures (6–0 chromic gut, Ethicon). Each ligation was approximately 1 mm apart. The thigh muscles were sutured shut with 6–0 braided black silk, and the skin was closed with surgical wound clips. Nociceptive behavioral tests: Mice were allowed to recover from peripheral nerve injury for approximately 1–2 weeks. The development of cold allodynia was measured by subjecting the animals injured hindpaw to acetone.³¹ Briefly, each animal was placed in an acrylic chamber that rested on an elevated wire mesh platform. Each animal was placed in the chamber and allowed to acclimate for 1 h. Using a 1 cm³ syringe and 23 gauge needle, 100 μ L of acetone was applied to the plantar surface of the injured hindpaw and measurements of pain behaviors (hind foot flinching, licking, and biting) were observed and recorded for 1 min after acetone application. Animals that did not display a baseline of more than 8 s of pain behaviors were omitted from the experiment.

Acknowledgment. We thank Xing Cheng for assistance with NMR spectroscopy and Christine Kao for assistance in NOS SAR-driving assays.

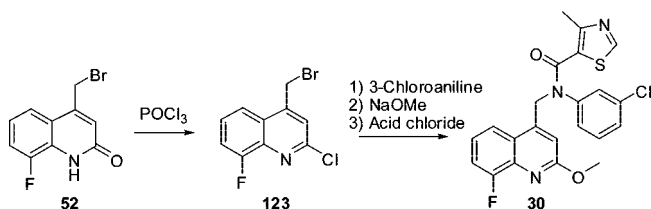
Supporting Information Available: Copies of the ¹H NMR, ¹³C NMR, LC trace, and high resolution mass spectrum. This material is available free of charge via the Internet at <http://pubs.acs.org>.

References

- (1) (a) Vallance, P.; Leiper, J. Blocking NO Synthesis: How, Where, and Why? *Nat. Rev. Drug Discovery* **2002**, *1*, 939–950. (b) Alderton, W. K.; Cooper, C. E.; Knowles, R. G. Nitric oxide synthases: structure, function and inhibition. *Biochem. J.* **2001**, *357*, 593–615.
- (2) Levy, D.; Zochodne, D. W. NO Pain: Potential Roles of Nitric Oxide in Neuropathic Pain. *Pain Pract.* **2004**, *4* (1), 11–18.
- (3) Paige, J. S.; Jaffrey, S. R. Pharmacologic Manipulation of Nitric Oxide Signaling: Targeting NOS Dimerization and Protein–Protein Interactions. *Curr. Top. Med. Chem.* **2007**, *7*, 97–114.
- (4) (a) Alderton, W. K.; Angell, A. D. R.; Craig, C.; Dawson, J.; Garvey, E.; Moncada, S.; Monkhouse, J.; Rees, D.; Russell, L. J.; Russell, R. J.; Schwartz, S.; Wasledge, N.; Knowles, R. G. GW274150 and GW273629 are potent and highly selective inhibitors of inducible nitric oxide synthase in vitro and in vivo. *Br. J. Pharmacol.* **2005**, *145*, 301–312. (b) Alba, D. A.; Clayton, N. M.; Collins, S. D.; Colthup, P.; Chessell, I.; Knowles, R. G. GW274150, a novel and highly selective inhibitor of the inducible isoform of nitric oxide synthase (iNOS), shows analgesic effects in rat models of inflammatory and neuropathic pain. *Pain* **2006**, *120*, 170–181.
- (5) Edwards, R. M.; Stack, E. J.; Trizna, W. Interaction of L-Arginine Analogs With L-Arginine Uptake in Rat Renal Brush Border Membrane Vesicles. *J. Pharmacol. Exp. Ther.* **1998**, *285*, 1019–1022.
- (6) Guthikonda, R. N.; Shah, S. K.; Pacholok, S. G.; Humes, J. L.; Mumford, R. A.; Grant, S. K.; Chabin, R. M.; Green, B. G.; Tsou, N.; Ball, R.; Fletcher, D. S.; Luell, S.; MacIntyre, D. E.; MacCoss, M. Bicyclic amidine inhibitors of nitric oxide synthase: discovery of perhydro-iminopyrindine and perhydro-iminoquinoline as potent, orally active inhibitors of inducible nitric oxide synthase. *Bioorg. Med. Chem. Lett.* **2005**, *15*, 1997–2001.
- (7) (a) LaBuda, C. J.; Koblisch, M.; Tuthill, P.; Dolle, R. E.; Little, P. J. Antinociceptive activity of the selective iNOS inhibitor AR-C102222 in rodent models of inflammatory, neuropathic and post-operative pain. *Eur. J. Pain* **2005**, *10* (6), 505–512. (b) Tinker, A. C.; Beaton, H. G.; Boughton-Smith, N.; Cook, T. R.; Cooper, S. L.; Fraser-Rae, L.; Hallam, K.; Hamley, P.; McNally, T.; Nicholls, D. J.; Pimm, A. D.; Wallace,

A. V. 1,2-Dihydro-4-quinazolinamines: Potent, Highly Selective Inhibitors of Inducible Nitric Oxide Synthase Which Show Antiinflammatory Activity in Vivo. *J. Med. Chem.* **2003**, *46* (6), 913–916.

- (8) (a) Davey, D. D.; Adler, M.; Arnaiz, D.; Eagen, K.; Erickson, S.; Guilford, W.; Kenrick, M.; Morrissey, M. M.; Ohlmeier, M.; Pan, G.; Paradkar, V. M.; Parkinson, J.; Polokoff, M.; Saionz, K.; Santos, C.; Subramanyam, B.; Vergona, R.; Wei, R. G.; Whitlow, M.; Ye, B.; Zhao, Z. S.; Devlin, J. J.; Phillips, G. Design, Synthesis, and Activity of 2-Imidazol-1-ylpyrimidine Derived Inducible Nitric Oxide Synthase Dimerization Inhibitors. *J. Med. Chem.* **2007**, *50*, 1146–1157. (b) Blasko, E.; Glaser, C. B.; Devlin, J. J.; Xia, W.; Feldman, R. I.; Polokoff, M. A.; Phillips, G. B.; Whitlow, M.; Auld, D. S.; McMillan, K.; Ghosh, S.; Stuehr, D. J.; Parkinson, J. F. Mechanistic Studies With Potent and Selective Inducible Nitric Oxide Synthase Dimerization Inhibitors. *J. Biol. Chem.* **2002**, *277*, 295–302.
- (9) Zhang, W.; Ramamoorthy, Y.; Kilcarslan, T.; Nolte, H.; Tyndale, R. F.; Sellers, E. M. Inhibition of Cytochromes P450 by Antifungal Imidazole Derivatives. *Drug Metab. Dispos.* **2001**, *30* (3), 314–318.
- (10) Choi, H. Y.; Chi, D. Y. Nonselective Bromination-Selective Debro-mination Strategy: Selective Bromination of Unsymmetrical Ketones on Singly Activated Carbon against Doubly Activated Carbon. *Org. Lett.* **2003**, *5* (4), 411–414.
- (11) Sullivan, P. T.; Norton, S. J. α -Bromo- and α -Chloropyridylalanines. *J. Med. Chem.* **1971**, *14* (6), 557–558.
- (12) Quin, L. D.; Russell, J. R.; Prince, R. D.; Shook, H. E. Double-Bond Migration in 1-Methyl-4-(carbethoxymethylene)phosphorinane. *J. Org. Chem.* **1971**, *36* (11), 1495–1499.
- (13) Compound **30** was independently prepared from 8-fluoroquinolinone **52** in four steps: Treatment with POCl₃ gave 2-chloroquinolinone **123**. 3-Chloroaniline was alkylated with **123**, followed by reaction with sodium methoxide to give the 2-methoxyquinoline. Acylation with 4-methylthiazole-5-carbonyl chloride then gave **30**.



- (14) Li, H.; McMillen, W. T.; Heap, C. R.; McCann, D. J.; Yan, L.; Campbell, R. M.; Munda, S. R.; King, C. R.; Dierks, E. A.; Anderson, B. D.; Britt, K. S.; Huss, K. L.; Voss, M. D.; Wang, Y.; Clawson, D. K.; Yingling, J. M.; Sawyer, J. S. Optimization of a Dihydropyridopyrazole Series of Transforming Growth Factor- β Type I Receptor Kinase Domain Inhibitors: Discovery of an Orally Bioavailable Transforming Growth Factor- β Receptor Type I Inhibitor as Antitumor Agent. *J. Med. Chem.* **2008**, *51* (7), 2302–2306.
- (15) Larock, R. C.; Babu, S. Synthesis of nitrogen heterocycles via palladium-catalyzed intramolecular cyclization. *Tetrahedron Lett.* **1987**, *28* (44), 5291–5294.
- (16) Vasselin, D. A.; Westwell, A. D.; Matthews, C. S.; Bradshaw, T. D.; Stevens, M. F. G. Structural Studies on Bioactive Compounds. 40.1. Synthesis and Biological Properties of Fluoro-, Methoxyl-, and Amino-Substituted 3-Phenyl-4H-1-benzopyran-4-ones and a Comparison of Their Antitumor Activities with the Activities of Related 2-Phenyl-benzothiazoles. *J. Med. Chem.* **2006**, *49* (13), 3973–3981.
- (17) The compound with the 3-pyridylamide was prepared with the 7,8-difluoroquinolinone: *N*-((7,8-difluoro-2-oxo-1,2-dihydroquinolin-4-yl)-methyl)-4-methyl-*N*-(pyridin-3-yl)thiazole-5-carboxamide-3-pyridyl (data not shown).
- (18) Symons, K. T.; Massari, M. E.; Nguyen, P. M.; Roppe, J.; Bonnefous, C.; Payne, J. E.; Smith, N. D.; Noble, S. A.; Sablad, M.; Rozenkrants, N.; Zhang, Y.; Rao, T. S.; Shiao, A. K.; Hassig, C. A. KLYP956 is a Non-imidazole-Based Orally Active Inhibitor of Nitric Oxide Synthase Dimerization. *Mol. Pharmacol.*, **2008**, submitted for publication.
- (19) SEITU (*S*-ethyl-isothiourea) is a non-selective, substrate competitive NOS inhibitor.
- (20) Data not shown.
- (21) Also compare to des-fluoroquinolinone analogue **35**, Table 4; hiNOS EC₅₀ = 0.17 mM.
- (22) Jackson, S. A.; Sahni, S.; Lee, L.; Luo, Y.; Nieduzak, T. R.; Liang, G.; Chiang, Y.; Collar, N.; Fink, D.; He, W.; Laoui, A.; Merrill, J.; Boffey, R.; Crackett, P.; Rees, B.; Wong, M.; Guillooteau, J.; Mathieu, M.; Rebello, S. S. Design, synthesis and characterization of a novel class of coumarin-based inhibitors of inducible nitric oxide synthase. *Bioorg. Med. Chem. Lett.* **2005**, *13*, 2723–2739.
- (23) Kato, H.; Negoro, M.; Wakabayashi, I. Effects of Acute Ethanol Administration on LPS-Induced Expression of Cyclooxygenase-2 and

- Inducible Nitric Oxide Synthase in Rat Alveolar Macrophages. *Alcohol.: Clin. Exp. Res.* **2005**, *29*, 285S–293S.
- (24) Wang, L. X.; Wang, Z. J. Animal and cellular models of chronic pain. *Adv. Drug Delivery Rev.* **2003**, *55*, 949–965.
- (25) Dubuisson, D.; Dennis, S. G. The Formalin Test: a Quantitative Study of the Analgesic Effects of Morphine, Meperidine, and Brain Stem Stimulation in Rats and Cats. *Pain* **1977**, *4*, 161–174.
- (26) When tested at a lower dose of 30 mg/kg po, compound **12** showed a reduction of phase II pain behaviors that did not reach significance. When dosed at 30 mg/kg ip, compound **12** gave a robust 86% reduction in phase II pain behaviors ($p < 0.01$).
- (27) (a) Bennett, G. J.; Xie, Y. K. A peripheral mononeuropathy in mouse that produces disorders of pain sensation like those seen in man. *Pain* **1998**, *33*, 87–107. (b) Joshi, S. K.; Hernandez, G.; Mikusa, J. P.; Zhu, C. Z.; Zhing, C.; Salyers, A.; Wismer, C. T.; Chandran, P.; Decker, M. W.; Honore, P. Comparison of Antinociceptive Actions of Standard Analgesics in Attenuating Capsaicin and Nerve-Injury Induced Mechanical Hypersensitivity. *Neuroscience* **2006**, *143*, 587–596.
- (28) De Laeter, J. R. Atomic Weights of the Elements. *Pure Appl. Chem.* **1991**, *63* (7), 975–990.
- (29) Vasselin, D. A.; Westwell, A. D.; Matthews, C. S.; Bradshaw, T. D.; Stevens, M. F. Structural studies on bioactive compounds. 40.1. Synthesis and biological properties of fluoro-, methoxyl-, and amino-substituted 3-phenyl-4*H*-1-benzopyran-4-ones and a comparison of their antitumor activities with the activities of related 2-phenylbenzothiazoles. *J. Med. Chem.* **2006**, *49* (13), 3973–3981.
- (30) Misko, T. P.; Schilling, R. J.; Salvemini, D.; Moore, W. M.; Currie, M. G. A fluorometric assay for the measurement of nitrite in biological samples. *Anal. Biochem.* **1993**, *214*, 11–16.
- (31) Walczak, J. S.; Beaulieu, P. Comparison of three models of neuropathic pain in mice using a new method to assess cold allodynia: The double plate technique. *Neurosci. Lett.* **2006**, *399*, 240–244.

JM900173B